Atmos. Chem. Phys. Discuss., https://doi.org/10.5194/acp-2018-1219
Manuscript under review for journal Atmos. Chem. Phys.
Discussion started: 30 November 2018

Atmospheric Chemistry and Physics Discussions

Interrelations between surface, boundary layer, and columnar aerosol properties over a continental urban site

Dongxiang Wang[1], Dominika Szczepanik[1], Iwona S. Stachlewska[1]

[1]University of Warsaw, Faculty of Physics, Institute of Geophysics, Warsaw, 02-093, Poland

Correspondence to: Iwona S. Stachlewska (iwona.stachlewska@fuw.edu.pl)

Abstract. PollyXT Raman Polarization Lidar observations were performed at the Remote Sensing laboratory in Warsaw (52.2109°N, 20.9826°E), Poland, in the framework of the European Aerosol Research Lidar Network (EARLINET) and the Aerosols, Clouds and Trace gases Research Infrastructure (ACTRIS). Data collected in July, August and September of 2013, 2015 and 2016 were analysed using the classical Raman approach. In total 202 sets of profiles of the particle extinction and backscatter coefficient, and linear particle depolarization ratio at 355 nm and 532 nm were derived for statistical investigations (EARLINET/ACTRIS Data Base). The main analysis was focused on intensive optical properties obtained within aerosol boundary layer (ABL). The interrelationships of different optical properties inside ABL are discussed for different periods: entire day, nocturnal time and sunrise/sunset time. In addition, the lidar derived boundary layer optical properties were compared with the columnar daytime aerosol properties derived from radiometer (MFR-7, PolandAOD-NET) and photometer (C318, AERONET). Relationships of these and surface in-situ measurements of particulate matter with an aerodynamic diameter < 10μm (PM_{10}) and < 2.5μm ($PM_{2.5}$) (WIOŚ Network) are investigated. Within boundary layer, the lidar derived optical properties (entire day, 202 sets) revealed the mean aerosol optical depth (AOD_{ABL}) of 0.27±0.17 at 355 nm and 0.15±0.10 at 532 nm; the mean Ångström exponent ($ÅE_{ABL}$) of 1.65±0.45; the mean lidar ratio (LR_{ABL}) of 49 ±16 sr at 355 nm and 41±15 sr at 532 nm; the mean linear particle depolarization ratio ($PLDR_{ABL}$) of 0.02±0.01 at 355 nm and 0.05±0.02 at 532 nm, the mean water vapour mixing ratio ($WVMR_{ABL}$) of 8.16±2.40 g/kg. Aerosol composition within ABL was assessed based on the derived properties interpreted with respect to values reported in literature and backward trajectories; it consisted either of pure urban anthropogenic pollution aerosols (~60%), its mixtures with biomass burning aerosols (< 12%), pollen (< 8%) or marine particles (< 6%). No significant contribution of mineral dust in boundary layer was found. In summer and early-autumn in Warsaw, the lidar derived aerosol boundary layer height (ABLH) and the columnar radiometer/photometer AOD_{CL} show negative correlations (-0.6 to -0.7), attributed to likely influence of smoke, pollution and dust suspended in aerosol layers in the free troposphere, while the ABLH and the lidar derived AOD_{ABL} exhibit positive correlation (~ 0.6), attributed in majority cases to local anthropogenic pollution. LR_{ABL} and surface fine to coarse mass ratio (FCMR) presents weak positive-correlation (~ 0.4) at nocturnal time, due to the higher(lower) occurrence of fine(coarse) particles at night. On the contrary, weak negative-correlation (~ -0.3) of LR_{ABL} and FCMR are present in sunrise/sunset time, for inverse occurrence of fine and coarse particles. A negative-correlation of

Atmos. Chem. Phys. Discuss., https://doi.org/10.5194/acp-2018-1219
Manuscript under review for journal Atmos. Chem. Phys.
Discussion started: 30 November 2018

PLDR$_{ABL}$ and FCMR (~ -0.4 at 355nm, -0.6 to -0.7 at 532nm) for all time period and no relation between PLDR$_{ABL}$ and ÅE$_{ABL}$ (~0.05) was found. Relation of AOD$_{ABL}$ and PM$_{10}$ reveals positive correlation (0.4 355; 0.5 532) for sunrise/sunset time, but no significant correlations found for AOD$_{ABL}$ and PM$_{2.5}$ (0.26 at 355; 0.16 at 532 nm). In general, a positive correlation of AOD$_{ABL}$ and LR$_{ABL}$ (stronger pronounced at 355nm) and a negative correlation ÅE$_{ABL}$ and LR$_{ABL}$ (stronger pronounced at 532nm) is observed. The ÅE$_{CL}$ values stay roughly between 1.0 and 2.0, while the ÅE$_{ABL}$ values range from 0.1 to 2.5, indicating a variety of particle sizes occurring inside ABL during summer and early-autumn period in Warsaw.

Keywords: lidar; aerosol boundary layer; aerosol optical properties; particulate matter

1 Introduction

Atmospheric aerosols play a significant role in local and global climate and weather change. Aerosols affect the earth radiative budget, as they interact with the incoming solar short-wave radiation and the outgoing terrestrial long-wave radiation. Depending on the aerosol type, they can scatter or absorb the radiation, thus causing warming or cooling the atmosphere locally, at the surface and at the top of atmosphere (Kaufman et al. 2002). The variety of aerosol sources, those of natural and anthropogenic origin, as well as the influence of diverse meteorological conditions on their characteristics and transport, lead to aerosol contents strongly variable in the troposphere. Accordingly to the Inter-governmental Panel on Climate Change (Stocker et al. 2013), the sparse and/or poorly-known information on aerosol temporal and spatial variability causes high uncertainty in the assessment of their influence on the global radiation budget. To improve forecasts of global climate change, it is essential to reduce these uncertainties. Aerosol properties are one of the important parameters in aerosol studies, being useful for radiative transfer, environment and health studies. Aerosol optical properties, size and composition are also important for aerosol-cloud-radiation interaction studies.

Air pollution is one of the major environmental issues in metropolitan areas due to its adverse effects on human health (Chen et al. 2008, Lelieveld et al. 2015). Strong emissions, e.g., from traffic, industry or heating, can drastically decrease air quality, particularly when the emitted pollutants are captured below an inversion and when meteorological conditions prevent an exchange of polluted and clean air, as reported by Juda-Rezler et al. 2006. In Europe, surface particulate matter with an aerodynamic diameter below 10μm (PM$_{10}$) is one of the most serious air quality problems (De Leeuw et al. 2001). As atmospheric aerosols also affect air quality, health and environment, joint studies of aerosol optical properties in combination with PM can improve our knowledge on atmospheric environment.

The knowledge on boundary layer characteristics and its dynamics, both related to ambient meteorological conditions, is helpful to model and predict mechanisms that matter in weather forecasting, air pollution and climate change studies (Barlage et al. 2016). Therefore, it is meaningful to acquire the knowledge of the ABL top height distribution along with the aerosol optical properties within the ABL.

Lidar techniques seem to be an optimal tool to provide height-resolved aerosol data products. Several lidar techniques are suitable for aerosol studies and in the last ten years rapid progress in laser technology, measurement techniques, and data

acquisition systems has contributed to a much wider use of these techniques also for aerosol monitoring, ranging from the simple elastic backscatter lidar / ceilometer networks (Flentje et al. 2010) to the most advanced multi-wavelength Raman lidar system networks (Baars et al. 2016). The European Aerosol Research Lidar Network (EARLINET; https://www.earlinet.org) conducts lidar observations and provides relevant sets of lidar data products stored in a comprehensive, quantitative, and statistically significant database for the aerosol distribution over Europe (Pappalardo et al. 2018). Quality assurance program (Freudenthaler et al. 2018) and lidar data evaluation algorithms (Böckmann et al 2004) have been developed and assessed at each lidar station, as well as during the lidar intercomparison campaigns (e.g. Wandinger et al. 2016) to meet accuracy standards desired in aerosol radiative forcing need. The unique data set of lidar observations conducted over Europe allows for classification of the aerosol type (e.g. Papagiannopoulos et al. 2018) The EARLINET network is an integral part of the Aerosols, Clouds and Trace gases Research Infrastructure (ACTRIS; https://www.actris.eu) - a pan-European initiative consolidating actions amongst European partners producing high-quality observations of aerosols, clouds and trace gases. As different atmospheric processes are increasingly in the focus of many societal and environmental challenges, such as air quality, health, sustainability and climate change, ACTRIS initiatives aim to contribute in the resolving of challenges by providing a platform for researchers to combine their efforts more effectively, and by providing observational data of aerosols, clouds and trace gases openly to other external users.

The aerosol optical properties derived for boundary layer from lidar have been studied in a statistical approach at several EARLINET sites in Europe (e.g. Mattis et al. 2004, Amiridis et al. 2005, Matthias et al. 2004, Sicard et al. 2011, Siomos et al. 2018). However, studies regarding extensive Raman-lidar derived sets of optical properties, such as wavelength dependent aerosol lidar ratios, optical depths, depolarization ratios, completed with Ångstrom exponent and water vapour content, as compared and interpreted against surface particulate matter and columnar optical properties of are still rare and based on a case study approach (Stachlewska et al. 2017b, 2018) .

In the framework of the EARLINET, extensive observations at a continental, urban site in Warsaw at the Remote Sensing Laboratory (RS-Lab) of the Institute of Geophysics at Faculty of Physics at University of Warsaw have been performed since July 2013. Within this paper the data products of this site published in the EARLINET/ACTRIS Data Base will be utilized (Earlinet Publishing Group, 2018).

The paper deals with the aerosol optical properties derived within boundary layer from the complex Raman-polarization lidar, obtained in atmospheric column by radiometer and sunphotometer, and with the particulate matter measurements at the surface. Study is designed to investigate relationships between boundary layer, columnar aerosol optical properties, water vapour and surface PMs, along with ABL height characteristics. In section 2, the instrumentation and datasets are described. Section 3 presents methodology of boundary layer height derivation and the aerosol optical properties retrieval approaches. Section 4 focuses on comparisons of different types of mean optical properties as derived within boundary layer and in the atmospheric column, PMs and ABLHs. Conclusions are given in section 5.

2 Instrumentation and data set

The PollyXT Raman polarization and water-vapor lidar (52.2109°N, 20.9826°E, 112 m a.s.l.) is located at the Remote Sensing Laboratory (RS-Lab, https://www.igf.fuw.edu.pl/en/instruments) of the Institute of Geophysics at the Faculty of Physics of the University of Warsaw, Poland. The RS-Lab conducts observations as a part of the European Aerosol Research Lidar Network (EARLINET, www.earlinet.org , Pappalardo et al. 2014), it provides regular measurements within the worldwide Polly.NET lidar network (www.polly.tropos.de , Baars et al. 2016) and within the National Aerosol Research Network PolandAOD-NET (www.polandaod.pl , supplement material in Markowicz et al. 2016).

Since July 2013, Polly XT lidar performs quasi-continuous 24/7 observations. Powerful laser pulses (180, 110 and 60 mJ) at 1064, 532 and 355 nm are emitted co-axially and vertically, with a 20 Hz repetition frequency, into the atmosphere. Detection is performed with a Newtonian telescope at 8-channels (so-called $2\alpha + 3\beta + 2\delta$ + WV), which enables determination of the particle extinction coefficient profiles (α) at 532 nm and 355 nm, the particle backscatter coefficient profiles (β) at 1064 nm, 532 nm and 355 nm, the particle linear depolarization ratio profiles (δ) at 532 and 355 nm, and water vapour mixing ratio (WV). The signals at all channels are recorded up to 48 km with standard 7.5 m vertical resolution in temporal steps of 30 s. Measured signals are affected by an incomplete geometrical overlap between the emitted laser beam and the full field of view of the lidar telescope, and therefore the signals in the range below 400m altitude are rejected from further evaluation. The incomplete overlap-range issue posed a first constrain on the selected dataset, i.e. constraining analyses to summer and early-autumn data. The lidar is described in a great detail in Engelmann et al 2016.

Quality checked profiles of optical properties are stored in the EARLINET/ACTRIS Data Base (www.earlinet.org). The statistical analysis covers profiles derived for EARLINET regular measurements (Mondays and Thursdays with ± 2 hours from zenith and sunset) and for dedicated measurements (e.g. diurnal cycles, special alert events). From Warsaw site, only cloud-screened profiles evaluated using the classical Raman-approach are feed into the Data Base. The profiles obtained for lidar observations in July, August and September in the year of 2013, 2015 and 2016 were analysed (2014 was excluded from analyses due to too sparse data availability). In total, 202 lidar profiles were collected for this study (denoted as contributing to *entire time*), whereby 79 profiles were obtained for *nocturnal time* (23:00-03:00 UTC) and 74 profiles were derived from dusk till sunrise (05:00-07:00 UTC) and sunset till down (18:00-20:00 UTC), here defined as the *sunrise/sunset or transition time*. The precise sunrise and sunset times are available via www.timeanddate.com/sun/poland/warsaw. Note, that only 49 profiles were available at daytime conditions (07:00-18:00 UTC), which was considered as too low number to consider separately category of *day time*, i.e. these profiles join category *entire time*. However, comparisons of the optical properties from lidar and photometer were done for a subset of the daytime profiles.

Multi-Filter Rotating Shadowband Radiometer (MFR-7; Yankee Environmental Systems) was used for continuous passive measurements at the RS-Lab in the frame of the PolandAOD-NET network activities. The instrument operates at six narrow-band channels (415, 500, 610, 675, 870 and 940 nm) and one broadband channel. It measures direct, diffuse and total solar radiation from which the spectrally resolved aerosol optical depth is obtained. In-situ calibration using the classic Langley

approach is applied on regular basis. Details on the instrument design and uncertainty analyses are reported in Harrison et al. 1994. Cloud-screened products used in this study are: $AOD_{CL}(415)$ and $AOD_{CL}(500)$ with uncertainty at the level of ±0.025., and $ÅE_{CL}(415/500)$ with uncertainty at the level of ±0.04. There is a threshold on the values of AOD_{CL} <0.03, being excluded from analyses.

Sunphotometer (CE318; CIMEL Electronique) was deployed for continuous observations at Polish Academy of Science Observatory in Belsk, located 25 km south-west of the RS-Lab in Warsaw. Passive measurements of direct and diffuse solar irradiance and sky radiance at the Earth's surface at nine wavelengths in a spectral range from 340 nm to 1640 nm are used for retrieval of AOD and ÅE. The data are calibrated once a year at PHOTONS/AERONET-EUROPE calibration centre (http://loaphotons.univ-lille1.fr) and processed by the Aerosol Robotic Network (AERONET, http://aeronet.gsfc.nasa.gov, Holben et al. 1998). Products used in this study: AERONET Level 2.0 cloud-screened $AOD_{CL}(380)$ and $AOD_{CL}(500)$ with uncertainty at the level of ±0.01., and $ÅE_{CL}(380/500)$ with uncertainty at the level of ±0.03. There is a threshold on the values of AOD_{CL} <0.03, being excluded from analyses.

Particulate matter concentrations for particles with an aerodynamic diameter of less than 2.5µm and 10µm (denoted $PM_{2.5}$ and PM_{10}, respectively) were measured at the air-quality monitoring site of the Warsaw Regional Inspectorate of Environmental Protection (WIOS) in Warsaw-Ursynow, located 7.5 km from the RS-Lab. The daily and hourly averaged data are visualised via http://sojp.wios.warszawa.pl/raport-dobowy-i-roczny. The data measurements conducted at the stations of State Environmental Monitoring are gathered in the Air-Quality database JPOAT 2,0 of the National Chief Inspectorate for Environmental Protection (GIOS). This official, calibrated datasets of PM2.5 & PM10 are accessible via http://powietrze.gios.gov.pl/pjp/archive.

The measurement uncertainty is below 30% for the hourly concentrations. Products used in this study: surface daily and hourly mean particulate matter concentrations for $PM_{2.5}$ and PM_{10}, and the fine-to-coarse mass ratio (FCMR), defined as $PM_{2.5}/(PM_{10}-PM_{2.5})$ (Zawadzka et al. 2013). FCMR > 1.5 denotes *fine particles* domination (diameter < 2.5µm); FCMR < 0.5 means *coarse particles* domination (diameter between 2.5 µm to 10 µm). Values in the range of 0.5 < FCMR< 1.5 indicate that fine and coarse particles are distributed approximately equally.

Note that the radiometer MFR-7 derived AOD, the sunphotometer C813 derived AOD and the in-situ measured PM values are averaged with corresponding time of the lidar-derived optical profiles available for given period for the Warsaw site in the EARLINET/ACTRIS Data Base.

The temperature, pressure, relative humidity, wind speed and direction at the surface (p_0, T_0, RH_0, V_0, $Vdir_0$), were measured by the weather transmitter WXT510 (Vaisala) mounted on the roof platform of the RS-Lab at 21 m above the ground's surface.

The atmospheric pressure (p), temperature (T) and relative humidity (RH) profiles are obtained from the radiosonde RS92 (Vaisala) launched at two World Meteorological Organization sites located in Poland: WMO 12374 station in Legionowo (52.40°N, 20.96°E, 96 m a.s.l., 25 km North of Warsaw) and WMO 12425 station in Wroclaw (51.78°N, 16.88°E, 122 m a.s.l., 300 km South-West of Warsaw). The noon and midnight radiosounding profiles (launch at 11:15 / 23:15 UTC,

duration of circa 1.5 h) were visualized and downloaded via the University of Wyoming Upper Air Data website (weather.uwyo.edu/upperair/sounding.html).

3 Methodology of lidar products retrieval

The atmospheric boundary layer is regarded as the lowest layer of the troposphere, being directly influenced by the Earth's surface and reacting quickly to the surface forcing. The atmospheric boundary layer under well-mixed conditions in summer and early-autumn can be characterized as a layer efficiently trapping aerosol particles in itself (as in comparison with winter boundary layer) and therefore, it is expected to be in significant relation with the lidar derived aerosol boundary layer height (ABLH). The latter is derived from the lidar elastic-scattering aerosol backscatter signal, relying on a higher aerosol load within the boundary layer than in the free troposphere. Wang et al. 2018 demonstrated that for the PollyXT lidar data in Warsaw ABLHs derived using the wavelet covariance transform method (WCT) give optimal results. The WCT calculations are applied for ABLH estimations as in Wang et al. 2018, with slight modification of the methodology: i) the dilation of 30 range-bins is applied on signals averaged over 7.5 m and 30 min; and ii) the ABLH is derived at all three elastic wavelengths (355, 532 and 1064 nm), and then averaged for a final result.

Lidar signals stored in the EARLINET/ACTRIS Data Base were evaluated using the classical Raman retrieval approach as in Baars et al. 2016 and the ±45 calibration method as in Engelmann et al. 2016. The water vapour was obtained as in Stachlewska et al. 2017a. For all analysed data products, low- and mid-altitude clouds are screened prior to the retrieval. The profiles of the particle extinction and backscattering coefficients, and particle linear depolarization ratio were averaged over 30-60 min and smoothed with running mean over 49 range-bins (length of single range-bin is 7.5m). The profiles of the water vapour mixing ratio were averaged over 30-60 min and 60 m with no smoothing applied. In lidar retrieval, the atmospheric profiles of p, T, RH obtained by RS92 at Legionowo or Waroclaw (depending on the approaching direction of the air-mass transport) were used.

After having determined ABLH, the mean values of different optical properties within the boundary layer are derived. However, for the incomplete overlap region, special care of the data in lowermost altitude range have to be applied. The lowest value of available particle extinction coefficient was assumed as representative down to the ground surface; this being commonly accepted approach in lidar studies, e.g. Matthias et al. 2004. Therefore, the mean extinction coefficient of the entire ABL is obtained by extrapolating the extinction profile with this value down to the ground. Similarly, the mean backscattering coefficient and the particle depolarization ratio of ABL. The PLDR profiles can be derived almost to the ground, however for the EARLINET/ACTRIS Data Base profiles are stored down to 400 m, so that extrapolation also here is required. The water vapour mixing ratio profiles were also extrapolated from 100m down to the ground.

Additionally, within ABL, the vertical distribution of the lidar ratio (LR_{ABL}) was derived as a ratio of the aerosol extinction to backscatter coefficient profiles at 355 and 532 nm, and then the mean LR_{ABL} are calculated. The vertical distribution of the Ångström exponent $ÅE_{ABL}(355/532)$ was computed by the means of using the profiles of aerosol extinction coefficient (not

AOD!) at 355 and 532 nm, then mean $ÅE_{ABL}$ is calculated. The aerosol optical depth (AOD_{ABL}) has been calculated by integrating the extrapolated aerosol extinction profile derived with the lidar at 355 and 532 nm. There is a threshold on the values of $AOD_{ABL}(355) < 0.05$ and $AOD_{ABL}(532) < 0.03$, being excluded from analyses. Stachlewska et al. 2018 reported the uncertainty of AOD_{ABL} at 355 and 532 nm derived from the Raman extinction coefficient profiles < 20%, the uncertainty of LR_{ABL} derived by extinction-to-backscattering coefficient ratios at 355 and 532 nm < 35%, and the uncertainty of $PLDR_{ABL}$ at 355 and 532 nm < 20% of derived value. The uncertainty of extinction-derived $ÅE_{ABL}(355/532)$ is < 30% The uncertainty of the ABLH retrieval from PollyXT lidar are of ±40 m (Wang et al. 2018).

Lidar ratio is used for aerosol type determination; roughly speaking, LR > 75sr indicate existence of particles related to biomass burning, 40-50 sr mineral dust, 50-60 sr anthropogenic pollution, and 20-30 sr marine particles.

Particle linear depolarization ratio (PLDR) is used as an indicator of atmospheric anisotropy and tracer of non-spherical particles; roughly speaking, low values of PLDR < 0.01 are regarded as due to spherical particles in the atmosphere (e.g. pollution) and values of PLDR in the range of 0.2-0.35 are characteristic for pure dust. Polluted dust values are lower, down to even 0.1. Values in range of 4-8 are regarded as for biomass burning aerosol), then for pollen ~0.1, and for pollution <0.2.

The Ångstrom exponent (ÅE) was used as an indicator of the size of atmospheric aerosols. Values of ÅE ≤ 1 indicate particle size distributions dominated by the coarse-mode aerosols (radii ≥ 0.5 μm, here called *large particles*) that are typically associated with dust and sea salt particles (Perrone et al. 2014). Values of ÅE ≥ 1.5 indicate size distributions dominated by the fine-mode aerosols (radii < 0.5 μm, here called *small particles*) that are associated with urban pollution (Perrone et al. 2014). Values within the range of 1< ÅE < 1.5 belong to accumulation-mode (here called *medium-size particles*) and are associated with biomass burning aerosol Janicka et al. 2017. Use of the ÅE nomenclature of *small, medium, and large* size particle is for clarity, as not to confuse them with the fine-to-coarse mass ratio (FCMR).

4 Results and discussion

Table 1 shows the mean extinction coefficient (α), backscatter coefficient (β), aerosol optical depth (AOD), lidar ratio (LR), particle linear depolarization ratio (PLDR) and Ångström exponent (ÅE) derived at 355 and 532 nm channels within the aerosol boundary layer (ABL) for the entire (ET), nocturnal (NT) and sunrise/sunset (TT) time during the selected measurement period (July-September, 2013, 2015, and 2016). Different mechanisms govern the sunset and sunrise conditions; the first driving development of convective boundary layer and the latter lessens convection and prone stratification with residual layer. As the developed ABLH algorithm determines the aerosol boundary layer top as a well-mixed layer, a nocturnal layer and/or a residual layer, for the sunrise/sunset time it is used for data interpretation. The mean ABLH was of 1.65±0.43 km for this period. For comparison, Wang et al. 2018 demonstrated, based on the 10-years data set, that the decadal mean ABLH in Warsaw exhibits a clearly higher value in summer than in other seasons, whereby the mean summer ABLH was of 1.24±0.64 km in 2013, 1.80±0.60 km in 2015 and 1.57±0.67 km in 2016.

The mean values of α_{ABL}, AOD_{ABL} and LR_{ABL} calculated at the two wavelengths are similar in entire and nocturnal time, while corresponding values in sunrise/sunset time are relatively higher than for the two other periods. This indicates that the convective mixing and the change of atmospheric conditions impact light extinction on aerosol particles within the ABL. In general, the mean $ÅE_{ABL}$ was high, indicating small-size particles. In nocturnal period, $ÅE_{ABL}$ values are higher than for the other periods, indicating that even smaller particles occur at the nighttime during summer and early-autumn in Warsaw, however this does not necessarily mean that pollution is intensifying at night, as it may be related to less intense traffic, lack of photo-smog, and cooling at the ground surface at night.

The frequency distribution plots for the AOD_{ABL}, LR_{ABL}, $ÅE_{ABL}$ derived at 355 and 532 nm and the FCMR derived for $PM_{2.5}$ and PM_{10} for the entire, nocturnal and sunrise/sunset times are shown in Figure 1. The mean AOD_{ABL} mainly ranges from 0.1-0.3 at both wavelengths during three periods. Above 80% of occurrence is attributed to $AOD_{ABL}(355)$ in the range of 0.1-0.5 and $AOD_{ABL}(532)$ of below 0.3. The values of mean $LR_{ABL}(355)$ and $LR_{ABL}(532)$ mainly distribute from 30 to 70 sr, which accounts for more than 75% of total data, whereby frequency distributions of both are very similar for the nocturnal time. The majority of the $ÅE_{ABL}(355/532)$ values are larger than 1.0 (more than 90% of total data), which indicates mid- and small-size particles ($\leq$ 500nm) within boundary layer. On the other hand, the FCMR values between 0.5 and 1.5 constitute around 70% of total data, indicating a more-less equal distribution fine and coarse particles of a size between 2.5 and 10 µm at the surface.

Amiridis et al. 2005, reported the 4-years mean AOD_{ABL} of 0.44±0.16 at 355 nm, and the mean LR_{ABL} of 49±25 at 355 nm in summer at Thessaloniki, Greece. According to Papayannis et al. 2008, this much higher value of $AOD_{ABL}(355)$ can be attributed to a significantly stronger impact of the summertime Saharan dust events on Thessaloniki than on Warsaw. Sicard et al. 2011, reported low AOD_{ABL} of 0.07±0.02 at 532 nm in Northeastern Spain, and explained it by the influence of sea-breeze on Barcelona area. Mattis et al. 2004. reported for Leipzig the 3-years mean $AOD_{ABL}(355)$ of 0.38 and $AOD_{ABL}(532)$ of 0.18, with the mean $LR_{ABL}(355)$ of 58 sr and $LR_{ABL}(532)$ of 53 sr, and the mean $ÅE_{ABL}(355/532)$ of 1.4. However, the $ÅE_{ABL}$ was of 1.8-2.2 in the upper boundary layer during summer in Leipzig (Matthis et al. 2004), which is higher than values derived in Warsaw, i.e. during summer slightly larger particles are observed in ABL in Warsaw as compared to Leipzig. Matthias et al. 2004, derived for Raman lidar observations at 10 EARLINET stations: the lowest AOD_{ABL} values in the northwestern (Aberystwyth) and the highest values in the southeastern Europe (Athens), which was again attributed to the impact of Saharan dust events on the aerosol distribution in Southern Europe.

Lidar ratio can be used for the aerosol type characterization. Alados-Arboledas et al. 2011, reported lidar ratios of fresh biomass-burning pollution plume were of 60–65sr at 355 nm and 532 nm at Granada. Müller et al. 2007, reported the lidar ratios of 45-60 sr with a mean value of 53 sr at 532 nm, and the particle depolarization ratio <0.05 for Leipzig under local and regional urban and anthropogenic haze conditions. Amiridis et al. 2005 reported for Tessaloniki, the continental aerosol for 4-year mean lidar ratio of 40-47 sr at 355 nm and Giannakaki et al. 2010, the biomass burning aerosols for 7-year mean lidar ratio of 70 sr at 355 nm. Optical properties of eight aerosol types were derived by Burton et al. 2012 , derived over North America for the urban aerosol (lidar ratio at 532 nm of 53-70 sr with particle depolarization ratio of 0.03-0.07), and for

the smoke particles (lidar ratio of 33-46 sr with particle depolarization ratio of 0.04-0.09). The LR of marine particles with value of 20-26 sr at 532 nm was found in North Atlantic and Tropical Indian Ocean by Müller et al. 2007, and 25±4 sr at 532 nm in Hawaii by Masonis et al.2003. Dawson et al. 2015 presented the global mean lidar ratio for marine aerosols to be 26 sr, with a range from 22±7 to 32±17 sr, depending on variation of mean ocean surface wind speed. Haarig et al. 2017 reported for the marine particles the lidar ratios varying from 19-27 at 355 nm and 23-25 at 532 nm, and particle depolarization ratio of 0.05-0.12 at 355 and 0.07-0.15 at 532 nm. In current study, for several cases LR_{ABL} in the range of 25-30 sr at both wavelengths were obtained (Fig.1), which indicates possible mixing of marine particles into the ABL in Warsaw during the analysed period.

Linear particle depolarization ratio is an indicator of non-spherical particles (Ansmann et al 2009, Sakai et al. 2010, Gasteiger & Freudenthaler. 2014). Generally, the total depolarization ratio in dust episodes are reported above 0.2, while anthropogenic pollution aerosols have a total depolarization ratio below 0.1 (Xie et al 2008, Nemuc et al. 2013). Heese et al. 2008 reported particle depolarization ratio for dust (~ 0.25) and biomass burning aerosol (< 0.1) over Sahel (West Africa). The particle depolarization ratios of dust particles in the range of 0.1-0.25 were reported in Leipzig (Matthis et al. 2004) and 0.3-0.35 at Ouarzazate, Morocco (Freudenthaler et al. 2009). The particle depolarization ratios of urban haze and fire smoke are reported of less than 0.05 at different sites (Müller et al. 2007). The particle linear depolarization ratio for marine aerosol in the range from 0.01 to 0.03 was reported by Groβ et al. 2011. In the current study, the results of the obtained $PLDR_{ABL}$ (shown in Fig.1) are within the range of the listed above values characterizing different aerosol types. As PLDR is sensitive to the size of the sensed non-spherical particles, in particular small-size particles (< 300 nm) sensed with twice larger wavelength can be under detection limit, as seen in Fig.1. Although, the dust cases were detected in the free troposphere during the given measurement period in Warsaw (e.g. Janicka et al. 2017), yet the derived PLDR values of entire observation time are less than 0.1, which means that no cases of pure dust particles deposited nor advected into the ABL, however polluted dust existence cannot be entirely excluded.

Overall, during period of July to September of 2013, 2015 and 2016 in Warsaw, the aerosol composition within the ABL consisted mainly of urban and anthropogenic aerosols. It was assessed based on derived properties ($ÅE_{ABL}$, $WVMR_{ABL}$ and wavelength dependent LR_{ABL} and $PLDR_{ABL}$), as interpreted with respect to values reported in literature and with the backward trajectories calculations (plots available via PolandAOD-NET website: www.polandaod.pl). Aerosol composition consisted either of i) pure urban anthropogenic pollution of local origin or transported from Czech Rep. via Silesia or and Germany (~60%), and with its mixtures with ii) grass and peatland biomass burning aerosols transported from Russia over Ukraine and Belarus (< 12%), iii) pollen emissions of strictly local origin form the many semi-natural Warsaw's parks (< 8%), iv) marine particles transport mainly from Arctic over Baltic Sea (< 6%). For remaining cases identification of aerosol composition was regarded as due to a mixture of more that tow sub-component. No significant contribution of mineral dust in boundary layer was found, although transport pathways from Sahara over Iberian Peninsula or via Italy were identified.

Figure 2 shows the daytime mean 30-60min average of the aerosol optical depth within aerosol boundary layer AOD_{ABL} at 355 and 532 nm, calculated from the mean extinction coefficient profiles of EARLINET PollyXT lidar in Warsaw. For

comparison, the columnar daytime mean 1h average (with threshold of at least 5 data points) of the AOD_{CL} at 380 and 500 nm determined from the AERONET C318 sun photometer observations in Belsk, as well as with the AOD_{CL} at 415 and 500 nm derived from the PolandAOD-NET MFR-7 radiometer measurements in Warsaw are plotted. Along with these three, Figure 2 depicts also the $ÅE_{CL}(380/500)$ computed from the AOD_{CL} of CIMEL, the $ÅE_{CL}(415/500)$ obtained from the AOD_{CL} of MFR-7, and extinction-derived $ÅE_{ABL}(355/532)$ of PollyXT. All products presented in Figure 2 were derived for period of July to September of 2013, 2015 and 2016, for these cases when all three instruments were conducting observations at the same time (i.e. 33 cases).

In Table 2, the C318 derived mean AOD is of 0.44±0.18 at 380 nm and 0.30±0.13 at 500 nm, the MFR-7 derived mean AOD is of 0.43±0.19 at 415 and 0.33±0.16 at 500 nm, and the PollyXT derived mean AOD_{ABL} is of 0.16±0.09 at 355 and 0.09±0.06 at 532 nm, for the 33 comparison points, respectively (Table 2). The columnar AOD_{CL} values of the two instruments are the same in the given uncertainty range, despite of the 25 km between the two sites! In general, it is expected that always $AOD_{ABL} < AOD_{CL}$ (e.g. Sicard et al. 2011). For a rural site roughly 80% of AOD_{CL} can be assumed as a proxy representative for AOD_{ABL}, e.g. Szczepanik & Markowicz 2018, which is however, not necessarily a valid assumption for the urban sites, e.g. Stachlewska et al. 2017, especially for conditions with high aerosol load in free troposphere, e.g. Janicka et al. 2017. The obtained results of the mean values of the AOD_{ABL} being 3-4 times lower than the mean values of AOD_{CL}, indicate that the aerosol layers in the free troposphere in summer and early-autumn over Warsaw, are likely occurring frequently and they significantly contribute to the sensed AOD_{CL}, which is very much in agreement with e.g. Markowicz et al. 2016. This is why, for comparisons in Table.2 in brackets, also the mean values derived for cases of no long-range transport in the free-troposphere, as given in EARLINET/ACTRIS Data Base (i.e. allocation to forest-fire, dust, etc.). Note that for the lack of free troposphere aerosol transport the obtained 3 year mean values of summer/early-autumn AOD_{ABL} of 0.2 at 355 nm and 0.1 at 532 nm are actually rather high values! For conditions with no aerosol layers in the free-troposphere about the site, Szczepanik & Markowicz, 2018 proposed an approximation of boundary layer aerosol load for rural mountainous site (Strzyzow, Poland) as being of AOD_{ABL} (Strzyzow) ≈ 80%AOD_{CL}. Clearly this approximation for Warsaw urban continental site would be rather of AOD_{ABL} (Warsaw) ≈ 67% AOD_{CL}.

In a closer look in Figure 2, the lidar derived AOD_{ABL} are of less than 0.05 on a few days, e.g. day 191, 9 July 2013), although both corresponding values of passive derived AOD_{CL} are more than 0.38. This is not a mistake. On 9 July 2013, the biomass burning aerosol from Canadian wildfires was detected by lidar in Warsaw, with an apparent optically thick aerosol layer suspended in the lower troposphere just above the boundary layer top height, as reported by Janicka et al. 2017 and Ortiz-Amezcua et al. 2017. Due to the low ABLH (< 1000 m) on this day, (not unusual under high pressure system over Poland e.g. Janicka & Stachlewska, Stachlewska et al 2018, the optical depth contribution of aerosol smoke layer in the free troposphere dominated over the optical depth contribution of the aerosol within boundary layer, which explains much higher columnar than boundary layer AOD. Markowicz et al. 2016, reported existence of aerosol layers in free troposphere with significant (up to 55%) contribution to the total optical depth, which is consistent with results obtained in the current paper.

In general, the results in Fig.2 obtained for the ÅE being related to particle size, show that retrievals by all three instruments have similar trend of variation with time. The $ÅE_{CL}$ values stay roughly between 1.0 and 2.0, while the $ÅE_{ABL}$ values range from 0.1 to 2.5, indicating a variety of particle sizes occurring inside ABL during summer and early-autumn period in Warsaw. In general, $ÅE_{ABL}$ and $ÅE_{CL}$ seem to be anti-correlated! The mean $ÅE_{CL}$ values given in Table 2, are the same, in the given variability range for all 33 cases, the differences being attributed also to different calculation wavelengths. The values in brackets (no long-range transport of aerosols in free-troposphere, show even higher $ÅE_{ABL}$ and $ÅE_{CL}$ mean values – indication for pollution constrained in boundary layer.

4.1 Relation of ABLH with optical properties and surface PM

The scatter plots of the mean AOD_{CL} and AOD_{ABL} against ABLH for the 33 comparison cases of collocated in time measurements conducted with the three instruments: C318, MFR-7 and PollyXT, are depicted in Figure 3. The AOD_{CL} and ABLH shows negative correlation, while the AOD_{ABL} and ABLH exhibits positive correlation; the latter, which is being in accordance with correlation coefficient of 0.55 between AOD_{ABL} and ABLH reported for Leipzig by Mattis et al. 2004 and for Warsaw by Stachlewska et al. 2017. On the other hand, during stationary high pressure system conditions over Poland, when there was no aerosol in free troposphere above Warsaw but it is injected into boundary layer, both AOD_{CL} and AOD_{ABL} can increase with increasing boundary layer height as e.g. on 24-29 August 2016 (Stachlewska et al. 2017b), even more clearly observed during 10-16 September 2016 (Stachlewska et al. 2018).

The opposite trend in AOD_{CL} – ABLH and AOD_{ABL} – ABLH, is expected to attribute to different type of aerosol load in free-troposphere and/or boundary layer. When aerosol layer containing particles of dust, smoke, pollution or their mixtures is suspended in the free troposphere, an increase of columnar AOD_{CL} values can be observed. Marinou et al. 2017 reported that dust particles can be transported far away from their source of origin and are frequently observed over central and northern Europe, with higher occurrences during summer. High occurrence of the dust particles over Warsaw in spring and summer was also reported by Chilinski et al. 2016 and Janicka et al. 2017. Biomass burning particles and smoke layers were detected over central Europe in summer of 2013 (Janicka et al. 2017, Ortiz-Amezcua et al. 2017, Trickl et al. 2015), of 2015 (Stachlewska et al. 2017b, Szkop & Pietruczuk 2017), and 2016 (Stachlewska et al 2018). The dust component and biomass burning were detected and analysed by Siomos et al. 2017, 2018 in south Europe with a long record of 10 years lidar dataset. The Canadian wildfire smoke detected in the troposphere and the stratosphere in summer 2017 over central Europe were reported by Haaring et al 2018 and Ansmann et al. 2018.

The less sufficient growth of the ABLH, can be explained as partly due to the fact that the aerosol layers suspended free troposphere will reduce the solar radiation reaching the surface and suppress the thermal turbulence, leading to lower boundary layer height. Several studies reported decreasing boundary layer height during occurrence of dust episodes Peraz et al. 2004, Alastuey et al. 2008, Pandolfi et al. 2013. Hence, for certain conditions the relationship of AOD_{CL} and ABLH can be expected to exhibit negative correlation.

The AOD_{ABL} is an integral of the extinction coefficient within ABLH and the ABLH is a variable of AOD_{ABL}, therefore ABLH is not expected to be strongly related with the aerosol conditions above in the free troposphere. Aerosol optical depth is unique parameter to determine the atmospheric aerosol load and the ABLH derived by lidar is relying on a higher aerosol concentration within the boundary layer than in the free troposphere. Therefore, a positive-correlation of AOD_{ABL} with ABLH, just as observed in Figure 3 can be expected. Note, that although an intrusion of biomass burning smoke into the ABL can contribute strongly to suppression of the growth of ABLH, as reported by Stachlewska et al. 2018, it still does not result in negative correlation.

The relationship of lidar derived AOD_{ABL}, $ÅE_{ABL}$ and ABLH at different time-period of the day are depicted in Figure 4. Since the AOD_{ABL} is related to the ABLH, then there is more aerosol load within the ABL, as compared to the free troposphere, and thus a positive-correlation of AOD and ABLH can be observed for the entire, nocturnal and sunrise/sunset times. For the entire observation period, the correlation coefficient of the ABLH with the AOD_{ABL} at 355 nm and 532 nm are of 0.66 and 0.63. A relatively high correlation coefficient (0.73) with standard deviation of only 0.0004 between ABLH and AOD_{ABL} at both wavelengths occurred in the sunrise/sunset time, while their correlation coefficients are weaker (at both wavelengths < 0.50) during the nocturnal time (residual layer effect), when aerosol load within ABL basically remain stable, due to much weaker vertical mixing at night.

The mean $ÅE_{ABL}$ is 1.65±0.45, indicating the domination of relatively small particles in the observation period. No obvious relationship between $ÅE_{ABL}$ and ABLH is obtained, however interestingly; a weak positive relation of them is captured in nocturnal time. This suggests that small particles ($ÅE_{ABL}$ > 1.5) dominated within ABL in/for an increasing nocturnal boundary height. (more pollution emitted or less humidity) This may be partly attributed to higher number of $PM_{2.5}$ emitted during the nocturnal time (17.32±7.47 μg/m^3), as compared to the other periods (15.45±7.83 μg/m^3 in the entire time and 15.07±8.81 μg/m^3 in the transition time). Note that given standard deviations indicate high variability of the obtained values.

Figure 5 illustrates the relationship between the ABLH, PM and FCMR. When the ABLH grows, a declining trend of FCMR can be observed, which is indicating an increase of coarse particles (number or/and size) at the surface with an ascending ABLH. In cannot be excluded that, adiabatic effects have partly influence on the growth of particle size. Schäfer et al. 2006 found a high negative correlation between PM_{10} and ABLH in Hanover and Munich in winter. Rost et al. 2009 reported a strong negative relationship between PM_{10} and ABLH in Stuttgart. Similarly, Du et al. 2013 find that $PM_{2.5}$ and ABLH exhibit negative correlation in Delhi and Xi'an. Geiß et al. 2017 reported that the link between the PM and ABLH can be attributed to several different reasons, such as meteorological conditions, terrain, local particle sources and even to the method of the ABLH retrieval itself. This was also confirmed for Warsaw by studies of long-range transported aerosol injections into the boundary layer by Stachlewska et al. 2017b, 2018. However, in general, no pronounced relationship between the PM and ABLH are expected for Warsaw, as in Zawadzka et al. 2013. Also in the current study, no significant link between particulate matter (PM_{10} and $PM_{2.5}$) and ABLH was found for Warsaw during summer and early-autumn (Figure 5), which at least partly can attributed to relatively low records of PM emissions (hourly values < 40 μg/m^3) and relatively high summer ABLHs (1-2.5 km). Clearly, the ABLH is not the main factor controlling the surface pollution in

summer in Warsaw, which is consistent with the reports by Bonn et al. 2016, Stachlewska et al. 2017b, 2018, and Geiß et al. 2017.

4.2 Interrelations within optical properties and with surface PM

The relationship of air pollution and aerosol optical properties are given in Figures 6 and 7. The separation thresholds are defined as FCMR > 1.5 (vertical line) means that fine particles (<2.5µm) dominated and FCMR < 0.5 (vertical dashed line) means domination of coarse particles (2.5-10µm). The ÅE roughly indicates dominating particle size distribution mode, with separation thresholds of for small particles ÅE > 1.5 (horizontal line) and large particles ÅE < 1 (horizontal dashed line). However, relationship between ÅE and aerosol size distribution is complicated, and so it is for the FCMR.

Figure 6 presents the relationship of $ÅE_{ABL}$, LR_{ABL}, $PLDR_{ABL}$ and surface FCMR for the entire time, nocturnal time and sunrise/sunset time during July, August and September in 2013, 2015 and 2016. Aerosol optical depth (AOD) not shown, as there is no clear correlation of AOD_{ABL} and FCMR (R^2<0.18 for all time periods; compare also Figure 7). In general, for all time periods the values of FCMR between 0.5 and 1.5 constitute the largest proportion in total (least for nocturnal time). In entire time the surface fine and coarse particles are almost equal but in nocturnal time there is more fine particles and at transition sunrise/sunset time there is more coarse particles. There is clear separation mark at FCMR of 1.5.

There is no correlation of $ÅE_{ABL}$ and FCMR for the entire time, however, a very weak negative correlation is visible for the nocturnal time and a very weak positive correlation for the sunrise/sunset time. For $1 < ÅE_{ABL} < 2$, this negative relationship at nocturnal time indicates more $PM_{2.5}$ and positive relationship at sunrise/sunset indicates more PM_{10} at the surface. Because of a weak vertical air motion (no convective mixing) and lower ABLH during the nighttime, relatively large aerosol particles are deposited in ABL and most of small aerosol particles stack below the inversion of boundary layer top (or residual layer). This should lead to an increase of number of small particles accumulated within nocturnal ABL, which manifest as fine particles increase at surface. In general, urban pollution, regarded as road traffic, industrial emission and chemical reaction of gases (SO_2, NO_2, NO_x), causes increase of both PM_{10} and $PM_{2.5}$ (He et al. 2008). The sunrise time (7:00-9:00 local time) corresponds to urban traffic emission, which can cause lifting of coarse particles from the ground, thus larger amounts of coarse particles can manifest (Zawadzka et al. 2013). Less traffic emission at nighttime, results in less PM_{10} and more $PM_{2.5}$ observed, therefore, an increasing FCMR appears (the mean PM_{10} data during measurement period was of 31.85±12.27 µg/m^3 in the nocturnal time, 33.36±12.90 µg/m^3 in the transition time, and 32,23 ±12.21 µg/m^3 in the entire time. PM2.5 was of 17.32±7.47 µg/m^3 at nocturnal time, 15.07±8.81 µg/m^3 in the transition time and 15.45±7.83 µg/m^3 in the entire time. Both less traffic emission and strong stratification at night are reasons for the observed differences). Note: $STD_{2.5}$ (~8-9) and STD_{10} (~12-13) are similar for all periods, thus values are the same within given uncertainty!

The relationship of LR_{ABL} and FCMR in Figure 6, shows no correlations for the entire time. However, there is a weak positive correlation at the nocturnal time, being mainly a result of higher abundance of the fine particles ($PM_{2.5}$ with higher

LR_{ABL} values 35-85sr). On the contrary, when more coarse particles (PM_{10} with higher LR_{ABL} values 40-85sr) occur at sunrise/sunset time, a weak negative correlation is present.

The relationship of $PLDR_{ABL}$ and FCMR in Figure 6, shows relatively high negative correlations (0.4-0.7; stronger at 532nm) for all of the predefined time periods. The higher the abundance of fine particles at the surface, the more spherical particles is within the ABL and/or the more isotropic the atmosphere. Opposite holds for the increase of coarse particles. Both trends are especially well visible at the nocturnal versus the sunrise/sunset time.

Bennouna et al. 2016, reported that a significant positive correlation of PM_{10} and AOD_{CL} and increasing correlation coefficient for daily, monthly and yearly averages, relays on the aerosol characteristics of the site. Zawadzka et al. 2013, reported a negative correlation between PM_{10} and AOD_{CL} for long-term monthly mean values in winter in Belsk and Warsaw, and a positive relation for unstable (meaning strong turbulent vertical mixing in summer) atmospheric condition in Warsaw. Relationship between optical properties and surface aerosol mass concentration depends on boundary layer processes, chemical composition, source regions, weather conditions and aerosol type, which is challenging to be characterized well by columnar AOD_{ABL} and surface PM_{10} mass concentrations alone, and thus in Figure 7, a relationship of AOD_{ABL} and PM_{10} and $PM_{2.5}$ is depicted. No significant differences in the relation of AOD_{ABL} with PM_{10} or $PM_{2.5}$ are reported in current study (strikingly similar PM_{10} and $PM_{2.5}$!). Stachlewska et al. 2018 discussed such daily mean surface PM_{10} and $PM_{2.5}$ increase with increase of the AOD_{ABL} for growing ABLH in August 2016 in Warsaw. Figure 7 exhibits a very weak correlation of AOD_{ABL} and PM_{10} for the entire time (similar reported by Filip & Stefan 2011), no significant linear correlation for the nocturnal time, while some positive correlation was observed for the sunrise/sunset time (similar reported by Zawadzka et al. 2013). The ABL in summer is primarily driven by intensive convective mixing; resulting in significantly higher ABLH than in other seasons (Wang et al. 2018). In summer, the ABL aerosol can be elevated by effective convection to the free troposphere, and thus lead to decrease of aerosol loading within ABL, as reported by e.g. He et al. 2008, Tian et al. 2017. The emission of PM_{10} in summer is lower than for the other seasons in Warsaw (Zawadzka et al. 2013). Even less urban emissions at night reduce the mass concentrations of surface PM_{10}, and at the same time the aerosol properties within ABL are relatively stable due to stable boundary layer in nighttime. Therefore, no apparent relationship can be observed in nocturnal time.

Interrelations of optical properties within ABL are given in Figure 8. A positive correlation of AOD_{ABL} and LR_{ABL} is observed for entire time (~0.6), whereby it is higher for nocturnal time (0.7-0.8) and lower for sunrise/sunset time (~0.4). The AOD_{ABL} and LR_{ABL} depend on extinction coefficient derived within the ABL, thus both values will increase when fine particle contribution increases and/or when there is an increase of the light absorption capability of the particles within the ABL, and vice versa. This result may be partly due to the presence of biomass burning particles inside the ABL, as e.g. in Stachlewska et al. 2018.

The relationship between $ÅE_{ABL}$ and LR_{ABL} shows negative correlation during the analysed measurement period (0.2-0.6). The captured $ÅE_{ABL}$ decrease with increasing LR_{ABL} can be related with larger size particles being injected into the ABL, particles growing in the ABL or indicate significant smoke contribution in composition of ABL aerosol. As for the latter, a

possible explanation could be that the aging smoke was present in the ABL, which would be in agreement with literature, e.g. correlations of -0.79 and -0.84 between LR_{ABL} and $ÅE_{ABL}$ found for smoke particles e.g. by Giannakaki et al. 2010 and Amiridis et al 2009. Also Stachlewska et al 2018 showed negative correlation of $ÅE_{ABL}$ and LR_{ABL} for smoke particles. Another explanation could be as due to the condensation of large organic molecules and particle coagulation from upper atmosphere into the ABL, as reported by e.g. Posfai et al. 2004 and Fiebig et al 2003.

Giannakaki et al. 2010 showed no significant correlation of LR_{ABL} and $ÅE_{ABL}$ for continental and urban aerosols, which are mainly related with anthropogenic pollution. Also, no relationship between $ÅE_{ABL}$ and LR_{ABL} was reported by Mattis et al. 2004 when anthropogenic particles dominated in Leipzig. Nevertheless, obtained in current paper results show that for the mixture of local urban anthropogenic aerosols in ABL and natural long-range transported aerosols into the ABL, the relationship of $ÅE_{ABL}$ and LR_{ABL} display an negative correlation during summer and early-autumn in Warsaw. At nighttime, due to weaker air convection, slightly higher correlation coefficient of LR_{ABL} and $ÅE_{ABL}$ are obtained (Figure 8).

4.3 Relations of optical properties and relative humidity

Relations between the surface relative humidity (RH_0) with surface PM_{10} and $PM_{2.5}$ and FCMR for entire, nocturnal and sunrise/sunset time were investigated. Additionally, nighttime relation between lidar derived water vapour mixing ratios ($WVMR_{ABL}$) and relative humidity (RH_{ABL}) with surface PM_{10} and $PM_{2.5}$ and FCMR as well as with lidar derived aerosol properties ($ÅE_{ABL}$, LR_{ABL} and $PLDR_{ABL}$) were searched for.

Generally, a weak positive correlation of RH_0 and $PM_{2.5}$ and a weak negative correlation of RH_0 and PM_{10} was revealed for each time period (Figure 9), which is in agreement with the results of Sharma et al. 2017. The RH and FCMR exhibit positive correlation, with significantly higher correlation coefficients of 0.67, 0.58 and 0.72 in the entire, nocturnal and transition time, respectively. Zhang et al. 2015 reported that high relative humidity led to high PM2.5 in Beijing. Li et al. 2017 showed that in summer urban environment, due to the hygroscopic effect on aerosols, an increase of relative humidity can lead to a growth of the fine particles $PM_{2.5}$, but not to a growth of PM_{10}, mainly attributed to the effects of wet scavenging under high summer rainfall. The mean relative humidity obtained in current study was higher in the nocturnal time (60.44%±10.63), than in the entire (52.45%±13.30) and in the sunset/sunrise time (44.18%±11.94). Gou et al. 2017 reported that high relative humidity favors accumulation of pollutants. Then the small particles have greater possibility to aggregate into relatively large particles at nighttime, and thus lower correlation coefficients for RH and $PM_{2.5}$ (and FCMR) are found for the nocturnal time.

Figure 10 presents a weak positive relationship of water vapour mixing ratio within ABL ($WVMR_{ABL}$) and $PM_{2.5}$, PM_{10} and FCMR in nocturnal time during July, August and September in 2013, 2015 and 2016 in Warsaw. The correlation of $WVMR_{ABL}$ and $PM_{2.5}$ is a little higher than $WVMR_{ABL}$ and PM_{10}, indicating that water vapour in ABL affects surface fine particles more than surface coarse particles. Unlike for the relationship of RH_0 and PM_{10} (Figure 9), the WVMR and PM_{10} exhibit a weak positive correlation. One reason for this may be the presence of anthropogenic particles inside the ABL, as

these hygroscopic particles absorb water vapour and its gradually increase in size. Furthermore, growth of particles resulted from coagulation of particles within ABL cannot be excluded (Fiebig et al. 2003).

Figure 11, depicts scatter plots of water vapour mixing ratio and aerosol optical properties in nocturnal boundary layer during July, August and September in 2013, 2015 and 2016. No clear relations found between $WVMR_{ABL}$ and AOD_{ABL}, AE_{ABL} and LR_{ABL} for nocturnal time during given measurement period in Warsaw. $PLDR_{ABL}$ and $WVMR_{ABL}$ show a negative trend (Figure 11) with the correlation coefficient of -0.49 at 355 nm and -0.23 at 532 nm. The hygroscopicity of particles increases with decreasing particle size Petters et al. 2009, and at the same time, the more fine particles the lower the PLDR (see Figure 6). Hence, increase of water vapour and presence of hygroscopic particles leads to decrease of depolarization. For occurrence of long-range transported aerosol of biomass burning, hygroscopic effects can be well captured with quasi-continuous profiling of water vapour (Stachlewska et al. 2017).

As such, the obtained extensive data set have a potential to be used for testing and interpreting results of aerosol typing algorithms, especially those needing sets of Raman-derived lidar products as they are using artificial neural network approaches for aerosol categorization (Nicolae et al. 2018).

5 Conclusions

The study of optical properties within ABL calculated at 355 and 532 nm based on EARLINET dataset on July, August and September during 2013, 2015 and 2016 in Warsaw was conducted. Interrelationships of different optical properties within ABL were discussed. In addition, the relationship of aerosol optical properties within ABL and PM were highlighted. The comparison of various parameters was analysed in three different periods (entire time, nocturnal time and sunrise/sunset time).

AOD_{ABL} and LR_{ABL} at both wavelengths at sunrise/sunset are relatively higher than for the other two periods, indicating that convective mixing, and change of atmospheric conditions impact light extinction on aerosol particles in the ABL. In nocturnal period, $ÅE_{ABL}$ values are higher than for the two remaining periods, suggesting smaller particles dominate at nighttime during summer time in Warsaw. Aerosols composition within ABL of summer and early-autumn in Warsaw, consists of urban anthropogenic pollution, biomass burning aerosols, marine particles and their mixtures. Comparison of AOD_{ABL} with columnar AOD_{CL}, found the latter significantly higher (3-4 times) when optically thick aerosol layers due to long-range transport of air-masses were observed above the ABL, and less than 2 times higher for cases with no aerosol layers in the free troposphere (but with presence of aloft pollution due to convection). The AOD_{CL} and ABLH are negatively correlated (-0.58 to -0.62), which can be attributed to the influence of either dust or smoke layers suspended in free troposphere. The AOD_{ABL} and ABLH exhibit positive correlation (~0.60) in observation period. There is no clear relationship between $ÅE_{ABL}$ and ABLH, nor is there clear correlation between $ÅE_{ABL}$ and FCMR, although, a very weak negative correlation 0.31 of the latter at nighttime time and a very weak positive correlation 0.27 of them at sunrise/sunset is discerned. Due to more fine particles in nighttime boundary layer, LR_{ABL} and FCMR reveals positive correlation, and on the

contrary, negative correlation of LR_{ABL} and FCMR is present, when more coarse particles occur at sunrise/sunset time. A negative-correlation of $PLDR_{ABL}$ and FCMR was found for all time-periods, which indicates higher sphericity of fine particles and thus higher isotropy of the atmosphere what consisting of fine particles. Reported in literature, different correlations obtained for AOD_{ABL} and PM_{10} are explained as due to complicated atmospheric and weather conditions. In summer and early-autumn in Warsaw, there is generally high-pressure systems that govern the dynamics of the atmosphere, there is significantly less traffic pollution (people on holidays, on bicycles), pollination of plants plays role. The relationship between AOD_{ABL} and PM_{10} reported here, displays positive correlation only at sunrise/sunset (at least at sunrise this can be due to traffic peaks). Due to less urban emissions (neither traffic nor domestic heating) and relatively stable boundary layer at nighttime, no apparent relationship of AOD_{ABL} with PM_{10} was observed. The AOD_{ABL} and LR_{ABL} depend on extinction coefficient derived inside the ABL, thus their positive correlation is observed. Relationship of $ÅE_{ABL}$ and LR_{ABL} reveals negative correlation. When ABLH grows, a declining trend of FCMR is observed, indicating an increase of coarse particle fraction. However, there is no clearly apparent link between PM_{10} or $PM_{2.5}$ and ABLH.

The obtained results contribute to increase of knowledge on variability of optical properties within the aerosol boundary layer at a continental site in central Europe.

Bottom line is that regular, automated observations with the NeXT generation PollyXT lidar conducted at the EARLINET site allow for such studies. The excellent capabilities of this lidar gave possibility to combine the derived within this preliminary study lidar results with other data sources (e.g. AERONET). Hypothesis for boundary layer aerosol properties interrelations were proposed and will be further verified with more lidar data of regular observations in Warsaw. What could be improved by enlarging the existing high-quality lidar data sample is investigation of subgrouping of aerosol properties that could provide statistically significant correlations. Further, more observations will allow for extension of search for differences to other seasons, daytime analyses, and distinguishing sunset from sunrise aerosol properties relationships. Finally, a separation of aerosol properties accordingly to aerosol content, i.e. pure urban versus its mixture with other aerosol types, would be possible (currently too little data in mixed categories) and estimation of their radiative effect.

Acknowledgments:

This research has been done in the frame of the Technical assistance for Polish Radar and Lidar Mobile Observation System (POLIMOS) funded by ESA-ESTEC Contract no. 4000119961/16/NL/FF/mg.

The PollyXT-Warsaw lidar was developed in a scientific collaboration of the Faculty of Physics, University of Warsaw (FUW) with the Institute of Tropospheric Research (TROPOS). This development was financed by the Polish Foundation of Science and Technology (FNTP-No. 519/FNITP/115/2010). We especially acknowledge colleagues of the PollyXT Lidar Group lead by Dietrich Althausen.

Authors acknowledge the Warsaw Regional Inspectorate of Environmental Protection WIOS-Warsaw for provision of the processed $PM_{2.5}$ and PM_{10} data, visualised at http://www.wios.warszawa.pl. The data were accessed via the Data Archive of the National Chief Inspectorate for Environmental Protection (GIOS) via http://powietrze.gios.gov.pl/pjp/archive.

We acknowledge Brent Holben for processing of the AERONET data (https://AERONETl .gsfc.nasa.gov); Aleksander Pietruczuk and Piotr Sobolewski of Institute of Geophysics at Polish Academy of Sciences for performing the AERONET measurements in Belsk; Phillippe Golub for performing instrument calibrations at the PHOTONS/AERONET-EUROPE calibration center, supported by ACTRIS-1 project funded within the European Union Seventh Framework Program (FP7/2007e2013) under Grant Agreement No.262254.

We acknowledge Krzysztof Markowicz for processing of the MFR-7 data within the Polish aerosol Research Network PolandAOD-NET (https://polandaod.pl). The MFR-7 radiometer was purchased within a grant No.1283/B/P01/2010/38 of the Polish Ministry of Science and High Education.

The EARLINET is currently supported by the ACTRIS-2 project, funded by the European Union Research Infrastructure Action under the H2020 specific program for Integrating and opening existing national and regional research infrastructures of European interest under Grant Agreement No. 654109 and No. 739530. The University of Warsaw participates in ACTRIS-2 project as an associate partner without funding.

Author Contributions:

I.S.Stachlewska wrote the paper, obtained funding for the research, came up with the study approach, designed methodology, and performed experiment, contributed to development of PollyXT-Warsaw lidar and lidar evaluation algorithms, took care of quality assurance of lidar measurements and data products, and holistically interpreted the lidar results with other data sources results (AERONET, PolandAOD-NET). D.Szczepanik contributed with calculation of the aerosol optical properties profiles (α, β, DR) and with their categorization for the EARLINET/ACTRIS Data Base. D.Wang contributed with extensive literature review, wrote the codes for the ABLH and the WV retrieval algorithms, and performed statistical analysis of the optical properties (AE, LR, DR, WVMR). All authors contributed with merit revisions of the paper.

Conflicts of Interest: The authors declare no conflict of interest.

References

Alados-Arboledas, L., Müller, D., Guerrero-Rascado, J., Navas-Guzmán, F., Pérez-Ramírez, D., and Olmo, F.: Optical and microphysical properties of fresh biomass burning aerosol retrieved by Raman lidar, and star-and sun-photometry, Geophys. Res. Lett, 38, **2011**.

Alastuey, A., Querol, X., Castillo, S., Escudero, M., Avila, A., Cuevas, E., Torres, C., Romero, P. M., Exposito, F. and García, O.: Characterisation of tsp and pm2. 5 at Izaña, and Sta. Cruz de tenerife (Canary Islands, Spain) during a Saharan dust episode (July 2002), Atmos. Environ., 39, 4715-4728, **2005**.

Amiridis, V., Balis, D., Kazadzis, S., Bais, A., Giannakaki, E., Papayannis, A., and Zerefos, C.: Four-year aerosol observations with a Raman lidar at Thessaloniki, Greece, in the framework of European Aerosol Research Lidar Network (EARLINET), J. Geophys. Res., 110, **2005**.

Amiridis, V., Balis, D., Giannakaki, E., Stohl, A., Kazadzis, S., Koukouli, M., and Zanis, P.: Optical characteristics of biomass burning aerosols over Southeastern Europe determined from UV-Raman lidar measurements, Atmos. Chem. Phys., 9, 2431-2440**, 2009**.

Ansmann, A., Tesche, M., Knippertz, P., Bierwirth, E., Althausen, D., Mueller, D., and Schulz, O.: Vertical profiling of convective dust plumes in Southern morocco during SAMUM, Tellus B: Chem. and Phys. Meteo., 61, 340-353, **2009**.

Ansmann, A., Baars, H., Chudnovsky, A., Mattis, I., Veselovskii, I., Haarig, M., Seifert, P., Engelmann, R., and Wandinger, U.: Extreme levels of Canadian wildfire smoke in the stratosphere over Central Europe on 21–22 August 2017, Atmos. Chem. Phys., 18, 11831-11845, **2018**.

Baars, H., Kanitz, T., Engelmann, R., Althausen, D., Heese, B., Komppula, M., Preißler, J., Tesche, M., Ansmann, A., and Wandinger, U, Lim, J.-H., Ahn, J. Y., Stachlewska, I. S., Amiridis, V., Marinou, E., Seifert, P., Hofer, J., Skupin, A., Schneider, F., Bohlmann, S., Foth, A., Bley, S., Pfüller, A., Giannakaki, E., Lihavainen, H., Viisanen, Y., Hooda, R. K., Pereira, S. N., Bortoli, D., Wagner, F., Mattis, I., Janicka, L., Markowicz, K. M., Achtert, P., Artaxo, P., Pauliquevis, T., Souza, R. A. F., Sharma, V. P., van Zyl, P. G., Beukes, J. P., Sun, J., Rohwer, E. G., Deng, R., Mamouri, R.-E., and Zamorano, F.: An overview of the first decade of Polly NET: An emerging network of automated Raman-polarization lidars for continuous aerosol profiling, Atmos. Chem. Phys., 16, 5111-5137, **2016**.

Barlage, M., Miao, S., and Chen, F.: Impact of physics parameterizations on high-resolution weather prediction over two Chinese megacities, J. Geophys. Res., 121, 4487-4498, **2016**.

Belegante, L., Bravo-Aranda, J. A., Freudenthaler, V., Nicolae, D., Nemuc, A., Ene, D., Alados-Arboledas, L., Amodeo, A., Pappalardo, G., D'Amico, G., Amato, F., Engelmann, R., Baars, H., Wandinger, U., Papayannis, A., Kokkalis, P., and Pereira, S. N.: Experimental techniques for the calibration of lidar depolarization channels in EARLINET, Atmos. Meas. Tech., 11, 1119-1141, https://doi.org/10.5194/amt-11-1119-2018, **2018.**

Bennouna, Y., Cachorro, V. E., Mateos, D., Burgos, M. A., Toledano, C., Torres, B. and de Frutos, A.: Long-term comparative study of columnar and surface mass concentration aerosol properties in a background environment, Atmos. Environ., 140, 261-272, **2016**.

Bonn, B., Schneidemesser, E. V., Andrich, D., Quedenau, J., Gerwig, H., Lüdecke, A., Kura, J., Pietsch, A., Ehlers, C., and Klemp, D.: Baerlin 2014–the influence of land surface types on and the horizontal heterogeneity of air pollutant levels in Berlin, Atmos. Chem. Phys., 16, 7785-7811, **2016**.

Böckmann, C., Wandinger, U., Ansmann, A., Bösenberg, J., Amiridis, V., Boselli, A., Delaval, A., De Tomasi, F., Frioud, M., and Grigorov, I. V.: Aerosol lidar intercomparison in the framework of the EARLINET project. 2. Serosol backscatter algorithms, Applied Optics, 43, 977-989, **2004**.

Burton, S., Ferrare, R., Hostetler, C., Hair, J., Rogers, R., Obland, M., Butler, C., Cook, A., Harper, D., and Froyd, K.: Aerosol classification using airborne high spectral resolution lidar measurements–methodology and examples, Atmos. Meas. Tech., *5*, 73-98, **2012**.

Chen, B. and Kan, H.: Air pollution and population health: A global challenge, Environmental health and preventive medicine, 13, 94, **2008.**

Chilinski M. T., Markowicz K. M., Zawadzka O., Stachlewska I. S., Kumala W., Petelski T., Makuch P., Westphal D. L., and Zagajewski B.: Modelling and Observation of Mineral Dust Optical Properties over Central Europe, Acta Geophysica, 64 (6) , 2550-2590 , doi:10.1515/acgeo-2016-0069, **2016**.

Dawson, K., Meskhidze, N., Josset, D., and Gassó, S.: Spaceborne observations of the lidar ratio of marine aerosols, Atmos. Chem. Phys., *15*, 3241-3255, **2015**.

De Leeuw, F., Sluyter, R., van Bruegel, P., Bogman, F., and van Aalst, R.: Air pollution by ozone in Europe in 1999 and the summer of 2000, Office for Official Publications of the European Communities, **2001**.

Du, C., Liu, S., Yu, X., Li, X., Chen, C., Peng, Y., Dong, Y., Dong, Z., and Wang, F.: Urban boundary layer height characteristics and relationship with particulate matter mass concentrations in Xi'an, Central China, aerosol, Air Qual. Res., 13, 1598-1607, **2013**.

The EARLINET publishing group 2000-2015.: *EARLINET All 2000-2015*. World Data Center for Climate (WDCC) at DKRZ. https://doi.org/10.1594/WDCC/EARLINET_All_2000-2015, **2018**.

Engelmann, R., Kanitz, T., Baars, H., Heese, B., Althausen, D., Skupin, A., Wandinger, U., Komppula, M., Stachlewska, I.S., Amiridis, V, Marinou, E., Mattis, I., Linné, H., and Ansmann, A.: The automated multiwavelength Raman polarization and water-vapor lidar PollyXT: The next generation, Atmos. Meas. Tech., 9, 1767-1784, **2016**.

Fiebig, M., Stohl, A., Wendisch, M., Eckhardt, S., and Petzold, A.: Dependence of solar radiative forcing of forest fire aerosol on ageing and state of mixture, Atmos. Chem. Phys., 3, 881-891, **2003**.

Filip, L. and Stefan, S.: Study of the correlation between the near-ground pm10 mass concentration and the aerosol optical depth. J. Atmos. Solar.-Terrestrial. Phys., 73, 1883-1889, **2011**.

Flentje, H., Heese, B., Reichardt, J., and Thomas, W.: Aerosol profiling using the ceilometer network of the German Meteorological Service, Atmos. Meas. Tech. Discuss, 3, 3643-3673, doi.org/10.5194/amtd-3-3643-2010, **2010**.

Freudenthaler, V., Linné, H., Chaikovski, A., Rabus, D., and Groß, S.: EARLINET lidar quality assurance tools, Atmos. Meas. Tech. Discuss., doi.org/10.5194/amt-2017-395, in review, **2018**.

Freudenthaler, V., Esselborn, M., Wiegner, M., Heese, B., Tesche, M., Ansmann, A., Müller, D., Althausen, D., Wirth, M., and Fix, A.: Depolarization ratio profiling at several wavelengths in pure Saharan dust during SAMUM 2006, Tellus B: Chem. and Phys. Meteo., 61, 165-179, **2009**.

Gasteiger, J. and Freudenthaler, V.: Benefit of depolarization ratio at λ= 1064 nm for the retrieval of the aerosol microphysics from lidar measurements, Atmos. Meas. Tech., 7, 3773-3781, **2014**.

Geiß, A., Wiegner, M., Bonn, B., Schäfer, K., Forkel, R., Schneidemesser, E. V.; Münkel, C., Chan, K. L., and Nothard, R.: Mixing layer height as an indicator for urban air quality?, Atmos. Meas. Tech., 10, 2969-2988, **2017**.

Groß, S., Tesche, M., Freudenthaler, V., Toledano, C., Wiegner, M., Ansmann, A., Althausen, D., and Seefeldner, M.: Characterization of Saharan dust, marine aerosols and mixtures of biomass-burning aerosols and dust by means of multi-wavelength depolarization and Raman lidar measurements during SAMUM 2, Tellus B: Chem. and Phys. Meteo., 63, 706-724, **2011**.

Giannakaki, E., Balis, D., Amiridis, V., and Zerefos, C.: Optical properties of different aerosol types: Seven years of combined Raman-elastic backscatter lidar measurements in Thessaloniki, Greece, Atmos. Meas. Tech., 3, 569-578, **2010**.

Guo, H., Wang, Y., and Zhang, H.: Characterization of criteria air pollutants in Beijing during 2014–2015. Environ. Res., 154, 334-344, **2017**.

Haarig, M., Ansmann, A., Gasteiger, J., Kandler, K., Althausen, D., Baars, H., Radenz, M., and Farrell, D. A.: Dry versus wet marine particle optical properties: RH dependence of depolarization ratio, backscatter, and extinction from multiwavelength lidar measurements during saltrace, Atmos. Chem. Phys., 17, 14199, **2017**.

Haarig, M., Ansmann, A., Baars, H., Jimenez, C., Veselovskii, I., Engelmann, R., and Althausen, D.: Depolarization and lidar ratios at 355, 532, and 1064 nm and microphysical properties of aged tropospheric and stratospheric Canadian wildfire smoke, Atmos. Chem. Phys., 18, 11847-11861, **2018**.

Harrison, L., Michalsky, J., and Berndt, J.: Automated multifilter rotating shadow-band radiometer: An instrument for optical depth and radiation measurements, Applied Optics, 33, 5118-5125, **1994**.

He, Q., Li, C., Mao, J., Lau, A. K. H., and Chu, D.: Analysis of aerosol vertical distribution and variability in Hong Kong, J. Geophys. Res., 113, **2008**.

Heese, B. and Wiegner, M.: Vertical aerosol profiles from raman polarization lidar observations during the dry season amma field campaign, J. Geophys. Res., 113, **2008**.

Holben, B. N., Eck, T. F., Slutsker, I., Tanré, D., Buis, J. P., Setzer, A., Vermote, E., Reagan, J. A., Kaufman, Y. J., and Nakajima, T., et al., AERONET-A federated instrument network and data archive for aerosol characterization. Remote Sens. Environ., 66, 1-16, **1998**.

Janicka, L., Stachlewska, I. S., Veselovskii, I., and Baars, H.: Temporal variations in optical and microphysical properties of mineral dust and biomass burning aerosol derived from daytime Raman lidar observations over Warsaw, Poland, Atmos. Environ., 169, 162-174, **2017**.

Juda-Rezler K., Reizer, M., and Oudinet, J.P.: Determination and analysis of PM10 source apportionment during episodes of air pollution in Central Eastern European urban areas: The case of wintertime 2006, Atmos. Environ., 45(36), 6557-6566, **2011**.

Kaufman, Y. J. , Tanré, D., and Boucher, O.: A satellite view of aerosols in the climate system, Nature, 419, 215, **2002**.

Lelieveld, J., Evans, J. S., Fnais, M., Giannadaki, D., and Pozzer, A.: The contribution of outdoor air pollution sources to premature mortality on a global scale, Nature, 525, 367, **2015**.

Li, X., Ma, Y., Wang, Y., Liu, N., and Hong, Y.: Temporal and spatial analyses of particulate matter (pm10 and pm2. 5) and its relationship with meteorological parameters over an urban city in Northeast China. Atmos. Res., 198, 185-193, **2017**.

Marinou, E., Amiridis, V., Binietoglou, I., Tsikerdekis, A., Solomos, S., Proestakis, E., Konsta D., Papagiannopoulos, N., Tsekeri, A., and Vlastou, G.: Three-dimensional evolution of Saharan dust transport towards Europe based on a 9-year EARLINET-optimized CALIPSO dataset, Atmos. Chem. Phys., 17, **2017**.

Markowicz, K., Chilinski, M., Lisok, J., Zawadzka, O., Stachlewska, I., Janicka, L., Rozwadowska, A., Makuch, P., Pakszys, P., and Zielinski, T.: Study of aerosol optical properties during long-range transport of biomass burning from Canada to Central Europe in July 2013, J. Aeros. Sci., 101, 156-173, **2016**.

Masonis, S. J., Anderson, T. L., Covert, D. S., Kapustin, V., Clarke, A. D., Howell, S., and Moore, K.: A study of the extinction-to-backscatter ratio of marine aerosol during the shoreline environment aerosol study, J. Atmos. Ocean. Techn., 20, 1388-1402, **2003**.

Matthias, V., Balis, D., Bösenberg, J., Eixmann, R., Iarlori, M., Komguem, L., Mattis, I., Papayannis, A., Pappalardo, G., and Perrone, M.: Vertical aerosol distribution over Europe: Statistical analysis of Raman lidar data from 10 European aerosol research lidar network (EARLINET) stations, J. Geophys. Res., 109, **2004**.

Mattis, I., Ansmann, A., Müller, D., Wandinger, U., and Althausen, D.: Multiyear aerosol observations with dual-wavelength Raman lidar in the framework of EARLINET, J. Geophys. Res., 109, **2004**.

Nicolae, D., Vasilescu, J., Talianu, C., Binietoglou, I., Nicolae, V., Andrei, S., and Antonescu, B.: A neural network aerosol-typing algorithm based on lidar data, Atmos. Chem. Phys., 18, 14511-14537, https://doi.org/10.5194/acp-18-14511-2018, **2018**.

Müller, D., Ansmann, A., Mattis, I., Tesche, M., Wandinger, U., Althausen, D., and Pisani, G.: Aerosol-type-dependent lidar ratios observed with Raman lidar, J. Geophys. Res., 112, **2007**.

Nemuc, A., Vasilescu, J., Talianu, C., Belegante, L., and Nicolae, D.: Assessment of aerosol's mass concentrations from measured linear particle depolarization ratio (vertically resolved) and simulations, Atmos. Meas. Tech., 6, 3243-3255, **2013**.

Ortiz-Amezcua, P., Guerrero-Rascado, J. L., Granados-Muñoz, M. J., Benavent-Oltra, J. A., Böckmann, C., Samaras, S., Stachlewska, I. S., Janicka, Ł., Baars, H., and Bohlmann, S.: Microphysical characterization of long-range transported biomass burning particles from North America at three EARLINET stations, Atmos. Chem. Phys., 17, 5931-5946, **2017**.

Pandolfi, M., Martucci, G., Querol, X., Alastuey, A., Wilsenack, F., Frey, S., O'Dowd, C., and Dall'Osto, M.: Continuous aerosol boundary layer observations in the coastal urban area of Barcelona during SAPUSS, Atmos. Chem. Phys., 13, 4983-4996, **2013**.

Papagiannopoulos, N., Mona, L., Amodeo, A., D'Amico, G., Gumà Claramunt, P., Pappalardo, G., Alados-Arboledas, L., Guerrero-Rascado, J. L., Amiridis, V., Kokkalis, P., Apituley, A., Baars, H., Schwarz, A., Wandinger, U., Binietoglou, I., Nicolae, D., Bortoli, D., Comerón, A., Rodríguez-Gómez, A., Sicard, M., Papayannis, A., and Wiegner, M.: An automatic observation-based aerosol typing method for EARLINET, Atmos. Chem. Phys., 18, 15879-15901, https://doi.org/10.5194/acp-18-15879-2018, 2018.

Papayannis, A., Amiridis, V., Mona, L., Tsaknakis, G., Balis, D., Bösenberg, J., Chaikovski, A., De Tomasi, F., Grigorov, I., and Mattis, I.: Systematic lidar observations of Saharan dust over Europe in the frame of EARLINET (2000–2002), J. Geophys. Res., 113, **2008**.

Pappalardo, G., Amodeo, A., Apituley, A., Comeron, A., Freudenthaler, V., Linné, H., Ansmann, A., Bösenberg, J., D'Amico, G., and Mattis, I.: EARLINET: Towards an advanced sustainable European aerosol lidar network. Atmos. Meas. Tech., 7, 2389-2409, **2014**. Pérez, C., Sicard, M., Jorba, O., Comerón, A., and Baldasano, J.M.: Summertime re-circulations of air pollutants over the north-eastern Iberian coast observed from systematic EARLINET lidar measurements in Barcelona, Atmos. Environ., 38, 3983-4000, **2004**.

Perrone, M. R., De Tomasi, F., and Gobbi, G.: Vertically resolved aerosol properties by multi-wavelength lidar measurements, Atmos. Chem. Phys., 14, 1185-1204, **2014**.

Petters, M. D., Carrico, C. M., Kreidenweis, S. M., Prenni, A. J., DeMott, P. J., Collett, J. L., and Moosmüller, H.: Cloud condensation nucleation activity of biomass burning aerosol, J. Geophys. Res., 114, **2009**.

Pósfai, M., Gelencsér, A., Simonics, R., Arató, K., Li, J., Hobbs, P.V., and Buseck, P.R.: Atmospheric tar balls: Particles from biomass and biofuel burning, J. Geophys. Res., 109, **2004**.

Rost, J., Holst, T., Sähn, E., Klingner, M., Anke, K., Ahrens, D. and Mayer, H.: Variability of pm10 concentrations dependent on meteorological conditions, Intern. J. Environ. Poll., 36, 3-18, **2009**.

Sakai, T., Nagai, T., Zaizen, Y., and Mano, Y.: Backscattering linear depolarization ratio measurements of mineral, sea-salt, and ammonium sulfate particles simulated in a laboratory chamber, Applied Optics, 49, 4441-4449, **2010**.

Sicard, M., Rocadenbosch, F., Reba, M., Comerón, A., Tomás, S., García-Vízcaino, D., Batet, O., Barrios, R., Kumar, D., and Baldasano, J.: Seasonal variability of aerosol optical properties observed by means of a Raman lidar at an EARLINET site over Northeastern Spain, Atmos. Chem. Phys., 11, 175-190, **2011**.

Siomos, N., Balis, D. S., Poupkou, A., Liora, N., Dimopoulos, S., Melas, D., Giannakaki, E., Filioglou, M., Basart, S., and Chaikovsky, A.: Investigating the quality of modeled aerosol profiles based on combined lidar and sunphotometer data, Atmos. Chem. Phys., 17, 7003-7023, **2017**.

Siomos, N., Balis, D. S., Voudouri, K. A., Giannakaki, E., Filioglou, M., Amiridis, V., Papayannis, A., and Fragkos, K.: Are EARLINET and AERONET climatologies consistent? The case of Thessaloniki, Greece, Atmos. Chem. Phys., 18, 11885-11903, **2018**.

Stachlewska, I. S., Costa-Surós, M., and Althausen, D.: Raman lidar water vapour profiling over Warsaw, Poland, Atmos. Res., 194, 258-267, **2017**.

Stachlewska, I.S., Zawadzka, O., and Engelmann, R.: Effect of heat wave conditions on aerosol optical properties derived from satellite and ground-based remote sensing over Poland, Remote Sensing, 9, 1199, **2017**.

Stachlewska, I. S., Samson, M., Zawadzka, O., Harenda, K. M., Janicka, L., Poczta, P., Szczepanik, D., Heese, B., Wang, D., and Borek, K. Tetoni, E., Proestakis, E., Siomos, N., Nemuc, A., Chojnicki, B.H., Markowicz, K.M., Pietruczuk, A., Szkop,

A., Althausen, D., Stebel, K., Schuettemeyer, D., and Zehner, C.: Modification of local urban aerosol properties by long-range transport of biomass burning aerosol, Remote Sensing, 10, 412, **2018**.

Stocker, T., Qin, D., Plattner, G., Tignor, M., Allen, S., Boschung, J., Nauels, A., Xia, Y., Bex, V., and Midgley, P.: IPCC, 2013: *Climate Change 2013: The Physical Science Basis. Contribution of Working Group I to the Fifth Assessment Report of the Intergovernmental Panel on Climate Change*, Cambridge Univ. Press, Cambridge, UK, and New York, 1535 pp., **2013**.

Szczepanik, D. and Markowicz, K.: The relation between columnar and surface aerosol optical properties in a background environment, Atmos. Poll. Res., 9, 246-256, **2018**.

Szkop, A. and Pietruczuk, A.: Analysis of aerosol transport over southern poland in august 2015 based on a synergy of remote sensing and backward trajectory techniques. J. Appl. Rem. Sens., 11, 016039, **2017**.

Schäfer, K., Emeis, S., Hoffmann, H., and Jahn, C.: Influence of mixing layer height upon air pollution in urban and sub-urban areas, Meteorologische Zeitschrift, 15, 647-658, **2006**.

Sharma, A., Mandal, T., Sharma, S., Shukla, D., and Singh, S.: Relationships of surface ozone with its precursors, particulate matter and meteorology over Delhi, J. Atmos. Chem., 74, 451-474, **2017**.

Tian, P., Cao, X., Zhang, L., Sun, N., Sun, L., Logan, T., Shi, J., Wang, Y., Ji, Y., and Lin, Y.: Aerosol vertical distribution and optical properties over China from long-term satellite and ground-based remote sensing, Atmos. Chem. Phys., 17, 2509-2523, **2017**.

Trickl, T., Vogelmann, H., Flentje, H., and Ries, L.: Stratospheric ozone in boreal fire plumes–the 2013 smoke season over Central Europe, Atmos. Chem. Phys., 15, 9631-9649, **2015**.

Wandinger, U., Freudenthaler, V., Baars, H., Amodeo, A., Engelmann, R., Mattis, I., Groß, S., Pappalardo, G., Giunta, A., D'Amico, G., Chaikovsky, A., Osipenko, F., Slesar, A., Nicolae, D., Belegante, L., Talianu, C., Serikov, I., Linné, H., Jansen, F., Apituley, A., Wilson, K. M., de Graaf, M., Trickl, T., Giehl, H., Adam, M., Comerón, A., Muñoz-Porcar, C., Rocadenbosch, F., Sicard, M., Tomás, S., Lange, D., Kumar, D., Pujadas, M., Molero, F., Fernández, A. J., Alados-Arboledas, L., Bravo-Aranda, J. A., Navas-Guzmán, F., Guerrero-Rascado, J. L., Granados-Muñoz, M. J., Preißler, J., Wagner, F., Gausa, M., Grigorov, I., Stoyanov, D., Iarlori, M., Rizi, V., Spinelli, N., Boselli, A., Wang, X., Lo Feudo, T., Perrone, M. R., De Tomasi, F., and Burlizzi, P.: EARLINET instrument intercomparison campaigns: overview on strategy and results, Atmos. Meas. Tech., 9, 1001-1023, https://doi.org/10.5194/amt-9-1001-2016, **2016.**

Wang, D. S., Stachlewska, I. S., Song, X., Heese, B., and Nemuc, A.: Annual, seasonal and diurnal variability of boundary layer over an urban continental site based on 10 years of active remote sensing observations in Warsaw, Remote Sensing, *in review*, **2018.**

Xie, C., Nishizawa, T., Sugimoto, N., Matsui, I., and Wang, Z.: Characteristics of aerosol optical properties in pollution and asian dust episodes over Beijing, China, Applied Optics, 47, 4945-4951, **2008**.

Zawadzka, O., Markowicz, K., Pietruczuk, A., Zielinski, T., and Jaroslawski, J.: Impact of urban pollution emitted in Warsaw on aerosol properties. Atmos. Environ., 69, 15-28, **2013**.

Zhang, H., Wang, Y., Hu, J., Ying, Q., and Hu, X.-M.: Relationships between meteorological parameters and criteria air pollutants in three megacities in china. Environ. Res., 140, 242-254, **2015**.

Atmos. Chem. Phys. Discuss., https://doi.org/10.5194/acp-2018-1219
Manuscript under review for journal Atmos. Chem. Phys.
Discussion started: 30 November 2018

Atmospheric Chemistry and Physics Discussions

TABLES

Table 1. Mean values of the aerosol optical properties derived within aerosol boundary layer (ABL) from PollyXT lidar at the EARLINET site in Warsaw for measurements at 355nm and 532 nm conducted in period of July-September of 2013, 2015, and 2016. Symbols denote particle extinction coefficient (α), particle backscatter coefficient (β), aerosol optical depth (AOD), lidar ratio (LR), particle linear depolarization ratio (PLDR) and Ångstrom exponent (ÅE).

Optical Properties	Entire time (ET) 24/7		Nocturnal time (NT) 23:00-3:00 UTC		Sunrise/sunset time (TT) 5:00-7:00 & 18:00-20:00 UTC	
	355 nm	532 nm	355 nm	532 nm	355 nm	532 nm
α_{ABL} (Mm-1)	159 ±76	85±45	159 ±77	85±49	165 ±69	88±39
β_{ABL} (Mm-1sr-1)	3.2±1.1	2.0±0.7	3.3±1.1	2.1±0.6	3.0±1.1	2.0±0.8
AOD_{ABL}	0.27±0.17	0.15±0.10	0.25±0.14	0.13±0.08	0.30±0.18	0.16±0.10
LR_{ABL} (sr)	49±16	41±15	47±13	39±14	55±16	45±15
$PLDR_{ABL}$	0.02±0.01	0.05±0.02	0.02±0.01	0.05±0.02	0.02±0.01	0.05±0.02
$ÅE_{ABL}$	1.65±0.45		1.75±0.43		1.62±0.45	

Atmos. Chem. Phys. Discuss., https://doi.org/10.5194/acp-2018-1219
Manuscript under review for journal Atmos. Chem. Phys.
Discussion started: 30 November 2018

Atmospheric Chemistry and Physics Discussions

Table 2. Mean aerosol optical depth (AOD) and Ångstrom exponent (ÅE) with standard deviations derived within boundary layer at 355 and 532 nm from PollyXT lidar at the EARLINET site in Warsaw, and in atmospheric column at 380 and 500 nm measured by C318 CIMEL at the AERONET site in Belsk and at 415 and 500 nm measured by from MFR-7 radiometer at the PolandAOD-NET site in Warsaw. Average is obtained for July-September of 2013,2015, 2016 for cases when all instruments operated simultaneously (33 cases). In brackets, the mean values derived for cases of no long-range transport in the free-troposphere, as given in EARLINET/ACTRIS Data Base.

	$AOD_{ABL}(355)$	$AOD_{CL}(380)$	$AOD_{CL}(415)$	$AOD_{CL}(500)$	$AOD_{ABL}(532)$	ÅE
AERONET		0.44±0.18 (0.29±0.06)		0.30±0.14 (0.18±0.03)		1.47±0.23 (1.63±0.09)
PolandAOD-NET			0.45±0.21 (0.25±0.05)	0.34±0.17 (0.19±0.04)		1.53±0.21 (1.74±0.04)
EARLINET	0.16±0.09 (0.15±0.06)				0.09±0.06 (0.07±0.03)	1.59±0.53 (1.81±0.56)

Atmos. Chem. Phys. Discuss., https://doi.org/10.5194/acp-2018-1219
Manuscript under review for journal Atmos. Chem. Phys.
Discussion started: 30 November 2018

Atmospheric Chemistry and Physics Discussions

FIGURES

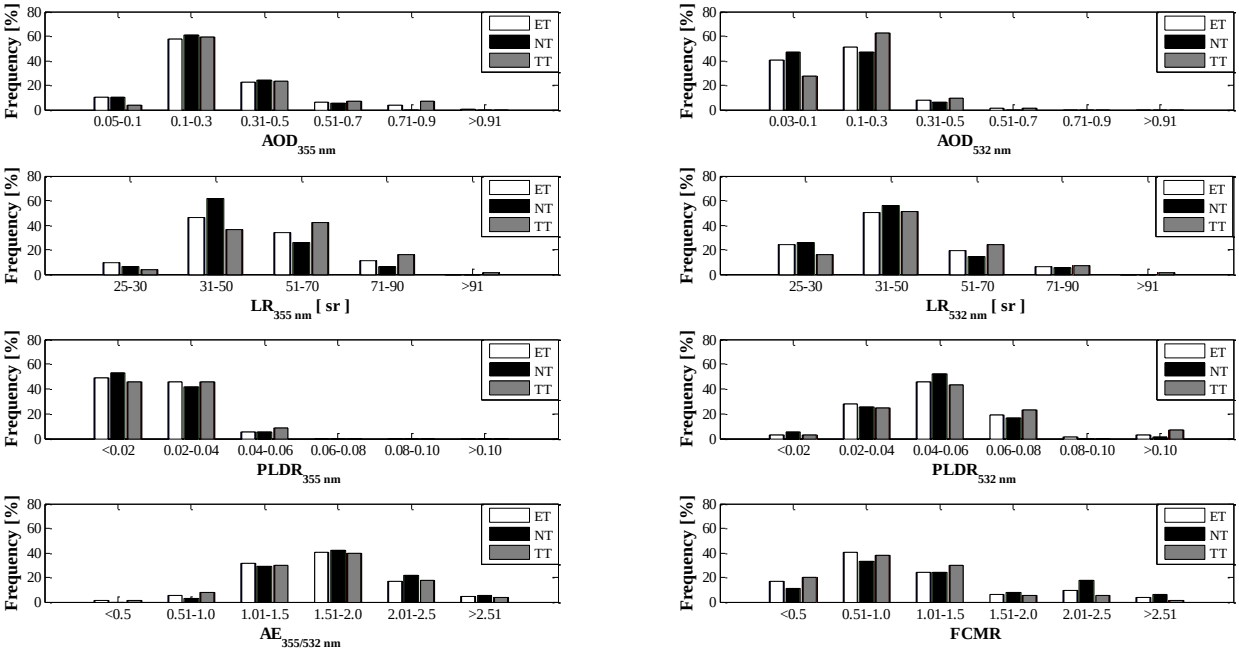

Figure 1. Frequency distribution of aerosol optical depth (AOD), lidar ratio (LR), particle linear depolarization ratio (PLDR) and Ångstrom exponent (ÅE) at 355 and 532 nm, derived within aerosol boundary layer at the EARLINET lidar site in Warsaw for period of July-September 2013, 2015, 2016 as compared to the fine to coarse mass ratio (FCMR) derived from surface particulate matter with an aerodynamic diameter below 10µm (PM_{10}) and below 2.5µm ($PM_{2.5}$) measurements at the WIOS site in Warsaw-Ursynów. The period of measurement is divided to the entire time (ET; 24 h), the nocturnal time (NT; 23:00-3:00 UTC) and the sunrise/sunset transition time (TT; 5:00-7:00 and 18:00-20:00 UTC).

Atmos. Chem. Phys. Discuss., https://doi.org/10.5194/acp-2018-1219
Manuscript under review for journal Atmos. Chem. Phys.
Discussion started: 30 November 2018

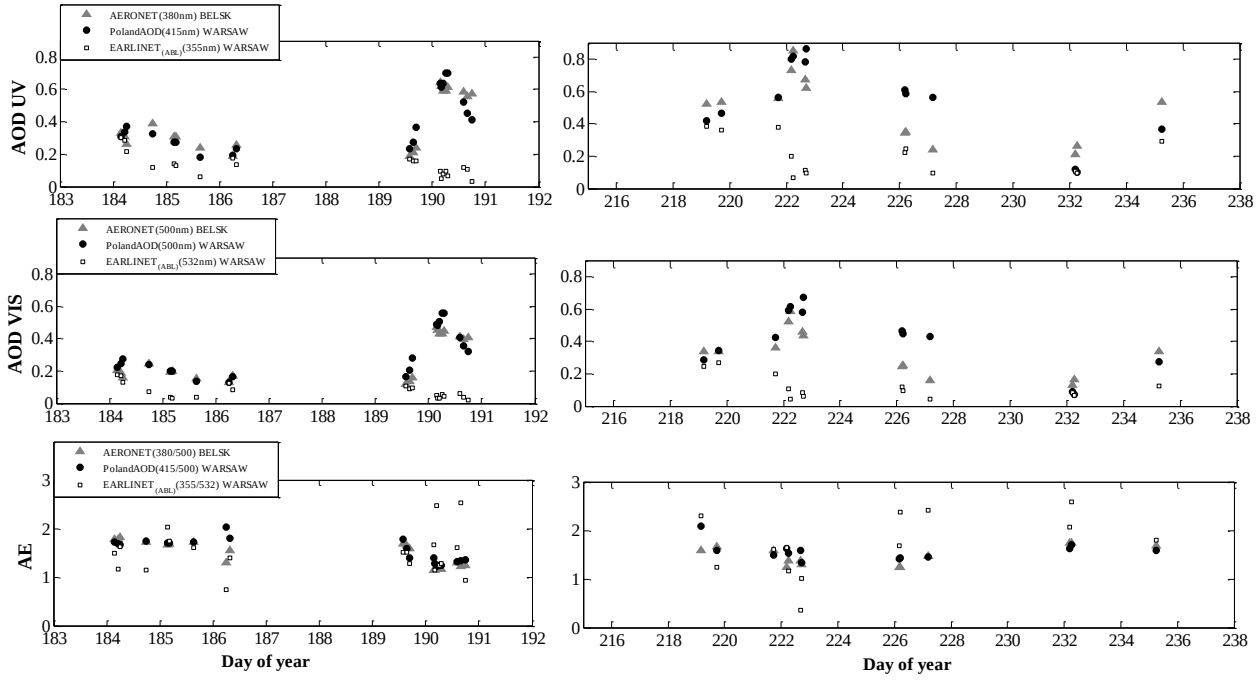

Figure 2. Hourly averages of aerosol optical depth (AOD) and Ångstrom exponent (ÅE) derived within boundary layer at 355 and 532 nm from PollyXT lidar at the EARLINET site in Warsaw (open circle/square), and in atmospheric column at 380 and 500 nm measured by C318 CIMEL at the AERONET site in Belsk (black/blue dots) and at 415 and 500 nm measured by from MFR-7 radiometer at the PolandAOD-NET site in Warsaw (grey/red dots). Note, only data points for which all 3 measurements were available are plotted. For day of year 182-274, for all years (2013,2015, 2016) we superimpose available data points (33 cases) on single plot (note 2016 was a lap year).

Atmos. Chem. Phys. Discuss., https://doi.org/10.5194/acp-2018-1219
Manuscript under review for journal Atmos. Chem. Phys.
Discussion started: 30 November 2018

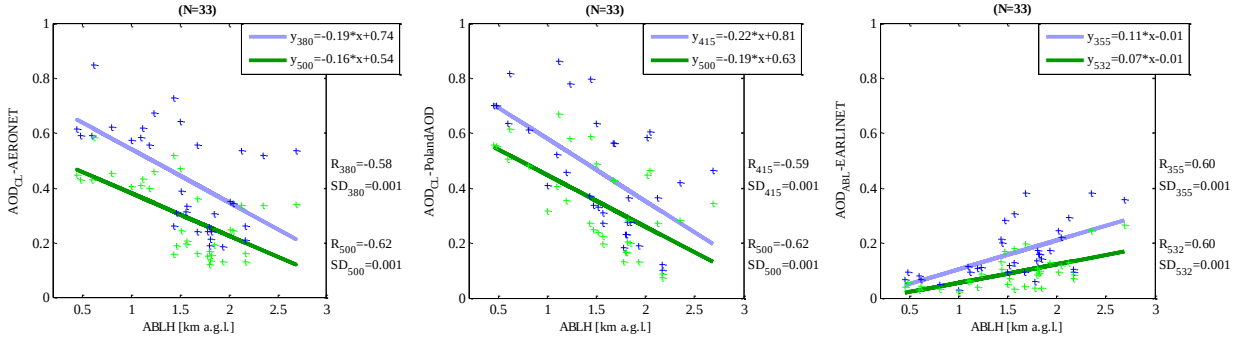

Figure 3. Comparison of hourly averaged aerosol optical depth (AOD) measured in atmospheric column at 380 and 500 nm by C318 CIMEL at the AERONET site in Belsk (left) and at 415 and 500 nm measured by from MFR-7 radiometer at the PolandAOD-NET site in Warsaw (middle) and derived within boundary layer at 355 and 532 nm from PollyXT lidar at the EARLINET site in Warsaw (right), against the lidar derived aerosol boundary layer height (ABLH) in Warsaw. Note, only data points for which all 3 measurements were available in period of July-September of 2013,2015, 2016 are plotted.

Atmos. Chem. Phys. Discuss., https://doi.org/10.5194/acp-2018-1219
Manuscript under review for journal Atmos. Chem. Phys.
Discussion started: 30 November 2018

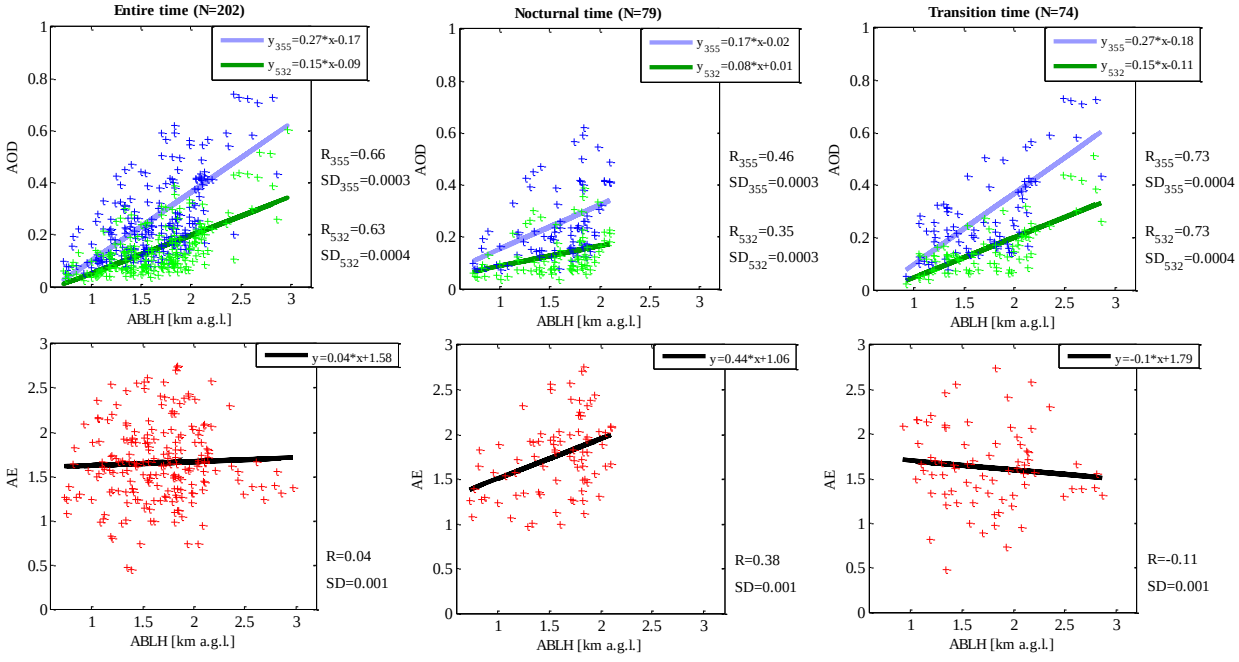

Figure 4. Comparison of hourly averaged aerosol optical depth (AOD) and Ångstrom exponent (ÅE) derived within boundary layer at 355 and 532 nm against aerosol boundary layer height (ABLH) derived from PollyXT lidar at the EARLINET site in Warsaw in period of July-September of 2013,2015, 2016.

Atmos. Chem. Phys. Discuss., https://doi.org/10.5194/acp-2018-1219
Manuscript under review for journal Atmos. Chem. Phys.
Discussion started: 30 November 2018

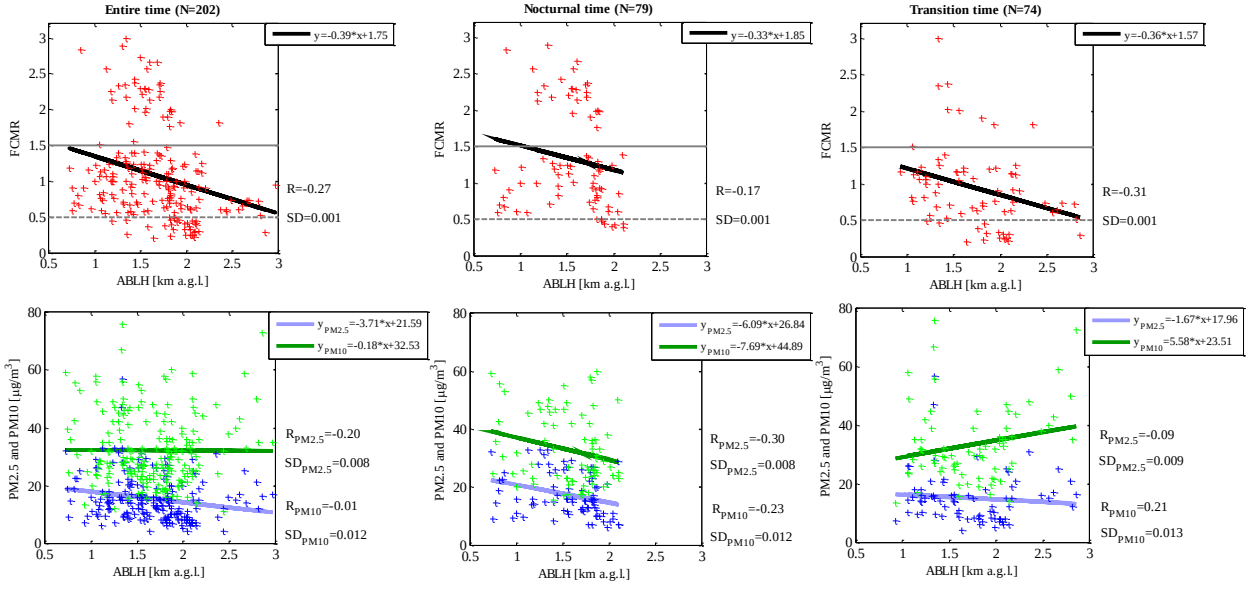

Figure 5. Comparison of hourly averages of surface fine to coarse mass ratio (FCMR), and particulate matter ($PM_{2.5}$ and PM_{10}) measured at the WIOS site in Warsaw-Ursynow with aerosol boundary layer height (ABLH) derived from PollyXT lidar at the EARLINET site in Warsaw in period of July-September of 2013,2015, 2016.

Atmos. Chem. Phys. Discuss., https://doi.org/10.5194/acp-2018-1219
Manuscript under review for journal Atmos. Chem. Phys.
Discussion started: 30 November 2018

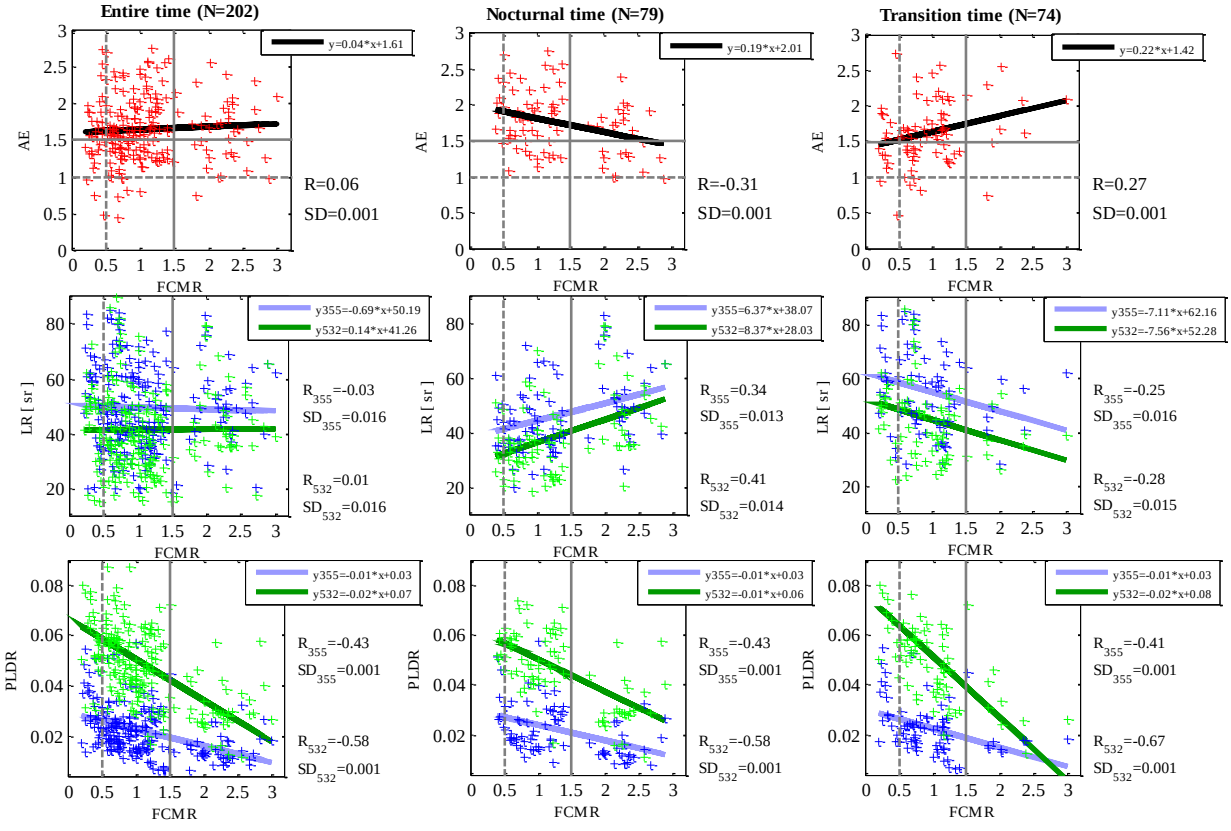

Figure 6. Comparison of hourly averaged Ångstrom exponent (ÅE), lidar ratio (LR) and particle linear depolarization ratio (PLDR) derived within boundary layer at 355 and 532 nm from PollyXT lidar at the EARLINET site in Warsaw in period of July-September of 2013,2015, 2016 with hourly averages of surface fine to coarse mass ratio (FCMR) derived from particulate matter ($PM_{2.5}$ and PM_{10}) measured at the WIOS site in Warsaw-Ursynow. Thresholds of AE and FCMR are marked as horizontal/vertical lines.

Atmos. Chem. Phys. Discuss., https://doi.org/10.5194/acp-2018-1219
Manuscript under review for journal Atmos. Chem. Phys.
Discussion started: 30 November 2018

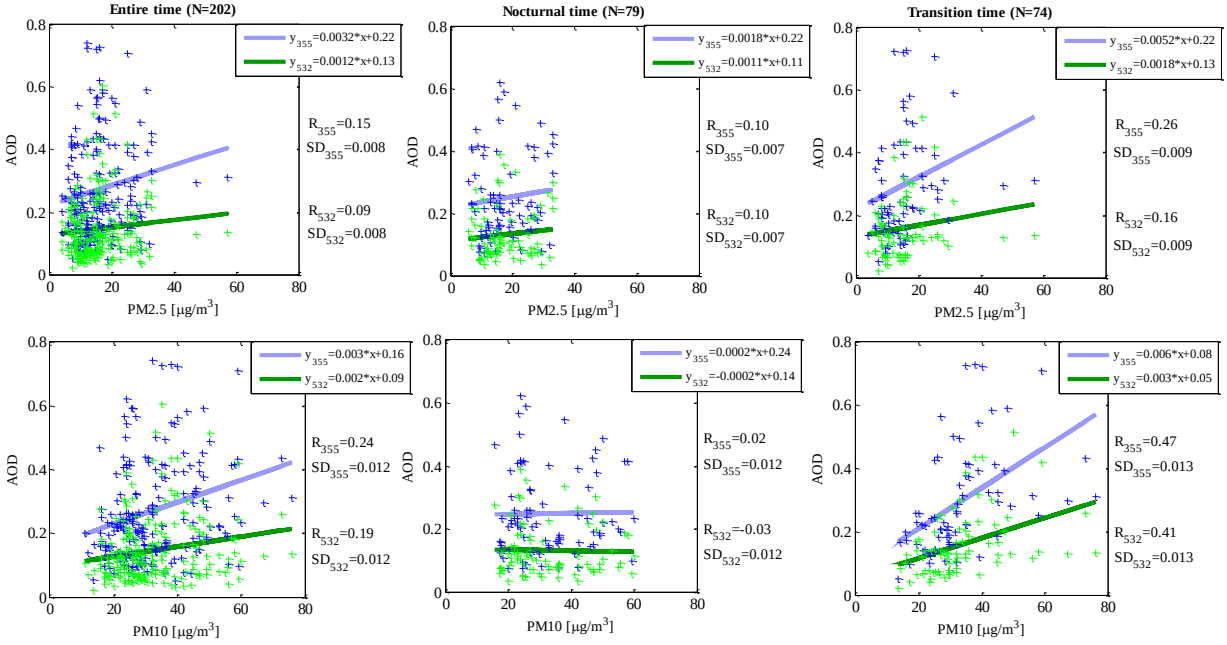

Figure 7. Comparison of hourly averaged aerosol optical depth (AOD) derived within boundary layer at 355 and 532 nm from PollyXT lidar at the EARLINET site in Warsaw in period of July-September of 2013,2015, 2016 with hourly averages of surface particulate matter ($PM_{2.5}$ and PM_{10}) measured at the WIOS site in Warsaw-Ursynow.

Atmos. Chem. Phys. Discuss., https://doi.org/10.5194/acp-2018-1219
Manuscript under review for journal Atmos. Chem. Phys.
Discussion started: 30 November 2018

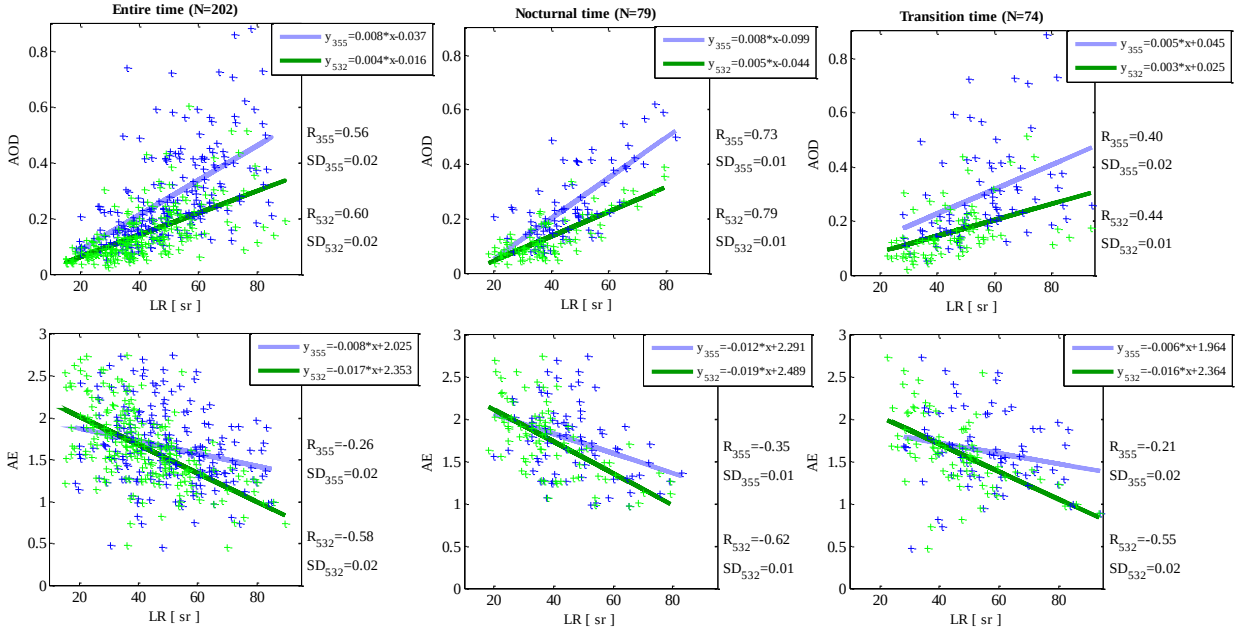

Figure 8. Comparison of hourly averaged aerosol optical depth (AOD), Ångstrom exponent (ÅE), and lidar ratio (LR) derived within boundary layer at 355 and 532 nm from PollyXT lidar at the EARLINET site in Warsaw in period of July-September of 2013,2015, 2016. The correlation of linear particle depolarization ratio (PLDR) and lidar ratio was of 0.01~0.04, not shown for brevity.

Atmos. Chem. Phys. Discuss., https://doi.org/10.5194/acp-2018-1219
Manuscript under review for journal Atmos. Chem. Phys.
Discussion started: 30 November 2018

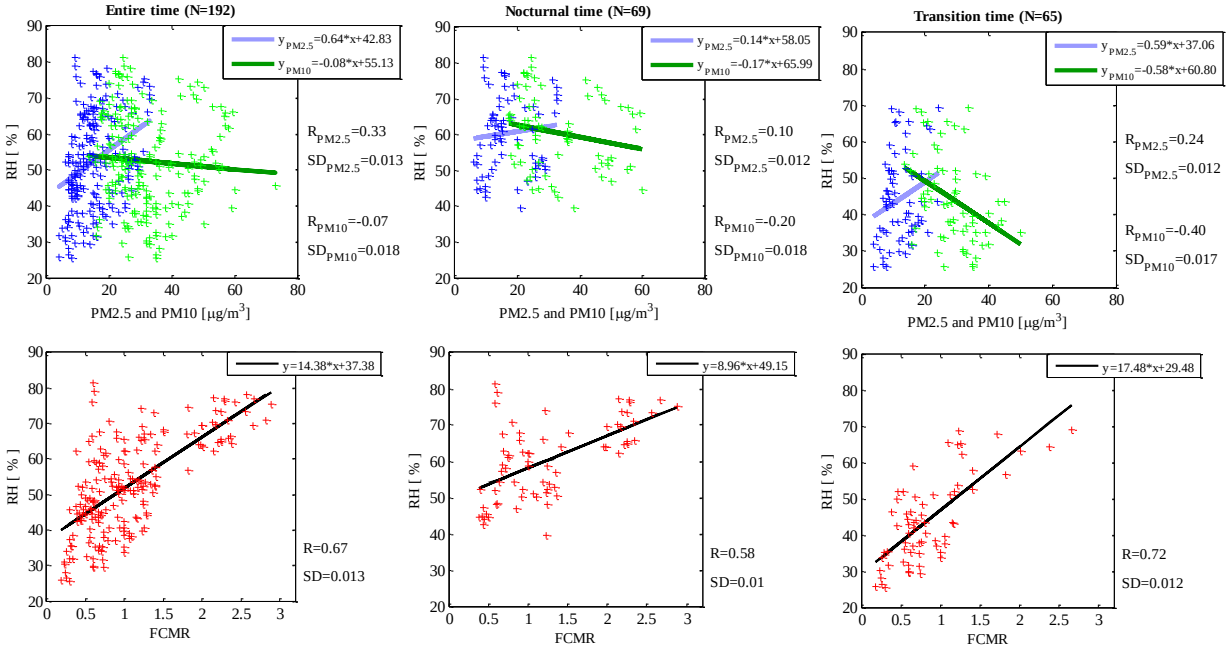

Figure 9. Comparison of the hourly averaged near-surface relative humidity (RH) measured by the weather transmitter WXT510 (Vaisala) in Warsaw in period of July-September of 2013,2015, 2016 with the hourly averages of surface particulate matter $PM_{2.5}$ and PM_{10} measured at the WIOS site in Warsaw-Ursynow.

Atmos. Chem. Phys. Discuss., https://doi.org/10.5194/acp-2018-1219
Manuscript under review for journal Atmos. Chem. Phys.
Discussion started: 30 November 2018

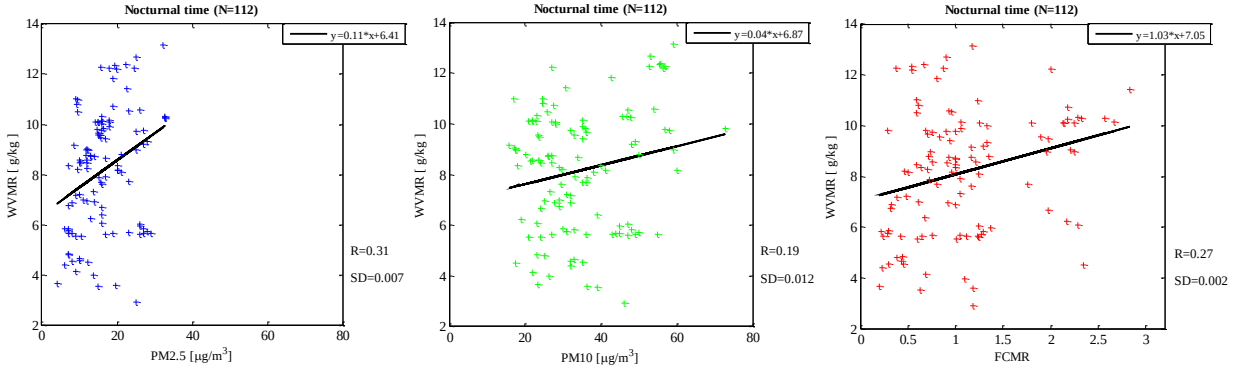

Figure 10. Comparison of the hourly water vapour mixing ratio (WVMR) derived within aerosol boundary layer at the EARLINET site in Warsaw at nocturnal time during period of July-September of 2013,2015, 2016 with the hourly averages of surface particulate matter $PM_{2.5}$ and PM_{10} measured at the WIOS site in Warsaw-Ursynow. NOTE: lidar water vapour available only at nighttime!

Atmos. Chem. Phys. Discuss., https://doi.org/10.5194/acp-2018-1219
Manuscript under review for journal Atmos. Chem. Phys.
Discussion started: 30 November 2018

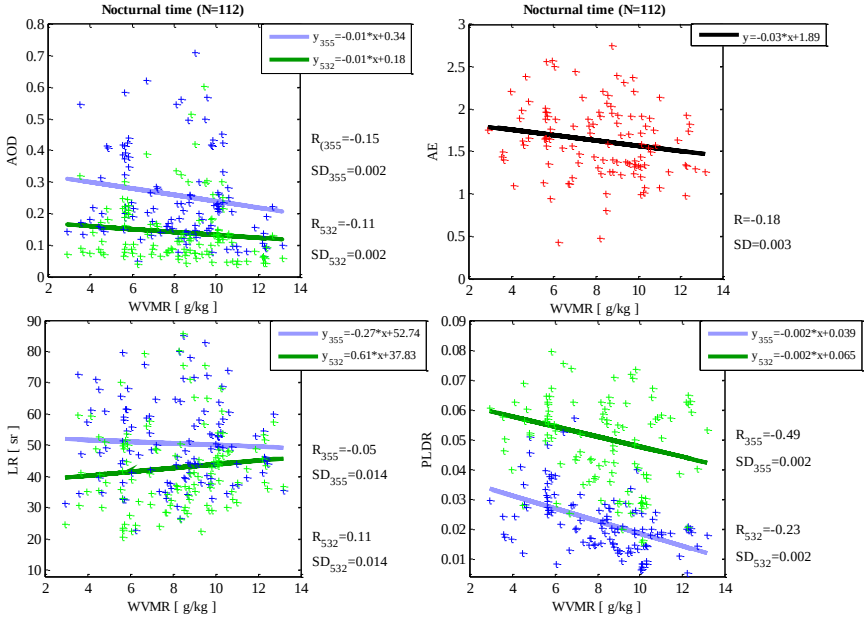

Figure 11. Comparison of Raman lidar nighttime hourly water vapour mixing ratio (WVMR), aerosol optical depth (AOD), lidar ratio (LR), Ångstrom exponent (ÅE) and particle linear depolarization ratio (PLDR) at 355 and 532 nm derived within aerosol boundary layer at the EARLINET site in Warsaw for July-September of 2013,2015, 2016.